Supplementary information

Extending cross metathesis to identify selective HDAC inhibitors: synthesis, modelling and biological activities.

Samuel Bouchet, Camille Linot, Dusan Ruzic, Danica Agbaba, Benoit Fouchaq, Joëlle Roche, Katarina Nikolic, Christophe Blanquart, Philippe Bertrand.

Table of Content

Molecular Formula Strings 2
Scheme S1 3
Syntheses 3
Table S1. Summary of current and previous CM results 6
^{1}H and ^{13}C NMR spectra 7
HPLC chromatograms 10
Biology 12
Figure S1. 14
Figure S2. 14
Figure S3. 15
Figure S4. 15
Figure S5. 15
Molecular Docking 16
Table S2. 16
Figure S6. 17
Figure S7 17
Figure S8 18
Figure S9 18
Figure S10 18
Figure S11 19
Figure S12 19
Figure S13 20
Figure S14 20
Figure S15 21
Figure S16 21
Figure S17 22
Figure S18 22
Figure S19 23
Figure S20 23
Figure S21 24
Atomic coordinates 24

Molecular Formula Strings

compound	SMILES
5	C=CCCC(=O)N(C(=O)OC(C)(C)C)OC(=O)OC(C)(C)C
6	C=CCCC(=O)Nc1ccccc1NC(=O)OC(C)(C)C
7	SC(c1ccccc1)(c1ccccc1)c1ccccc1
8	C=CCCCSC(c1ccccc1)(c1ccccc1)c1ccccc1
9	C(C/C=C/CCCSC(c1ccccc1)(c1ccccc1)c1ccccc1)CSC(c1ccccc1)(c1ccccc1)c1ccccc1
10	OC(=O)c1ccc2c(c1O)cccc2
11	COC(=O)c1ccc2c(c1O)cccc2
12	C=CCCCOc1c(ccc2c1cccc2)C(=O)OC
13	COC(=O)c1ccc2c(c1OCCC/C=C/CCCOc1c(ccc3c1cccc3)C(=O)OC)cccc2
14	COC(=O)c1ccc2c(c1OCCC/C=C/CCC(=O)N(C(=O)OC(C)(C)C)OC(=O)OC(C)(C)C)cccc2
15	COC(=O)c1ccc2c(c1OCCC/C=C/CCC(=O)Nc1ccccc1NC(=O)OC(C)(C)C)cccc2
16	COC(=O)c1ccc2c(c1OCCC/C=C/CCCSC(c1ccccc1)(c1ccccc1)c1ccccc1)cccc2
17	COC(=O)c1ccc2c(c1OCCCCCCCCC(=O)N(C(=O)OC(C)(C)C)OC(=O)OC(C)(C)C)cccc2
18	ONC(=O)CCCCCCCCOc1c(ccc2c1cccc2)C(=O)OC
19	COC(=O)c1ccc2c(c1OCCCCCCCCC(=O)Nc1ccccc1NC(=O)OC(C)(C)C)cccc2
20	COC(=O)c1ccc2c(c1OCCCCCCCCC(=O)Nc1ccccc1N)cccc2
21	COC(=O)c1ccc2c(c1OCCCCCCCCCSC(c1ccccc1)(c1ccccc1)c1ccccc1)cccc2
22	SCCCCCCCCCOc1c(ccc2c1cccc2)C(=O)OC
23	C=CCCC(=O)NCCc1c[nH]c2c1cccc2
24	C=CCCC(=O)NCCc1cn(c2c1cccc2)C
25	O=C(CC/C=C/CCC(=O)NCCc1cn(c2c1cccc2)C)NCCc1cn(c2c1cccc2)C
26	O=C(CC/C=C/CCC(=O)N(C(=O)OC(C)(C)C)OC(=O)OC(C)(C)C)NCCc1cn(c2c1cccc2)C
27	O=C(NCCc1cn(c2c1cccc2)C)CC/C=C/CCC(=O)Nc1ccccc1NC(=O)OC(C)(C)C
28	O=C(NCCc1cn(c2c1cccc2)C)CC/C=C/CCCSC(c1ccccc1)(c1ccccc1)c1ccccc1
29	O=C(NCCc1cn(c2c1cccc2)C)CCCCCCC(=O)Nc1ccccc1NC(=O)OC(C)(C)C

Scheme S1.

Preparation of the tryptaminoyl series.[a]

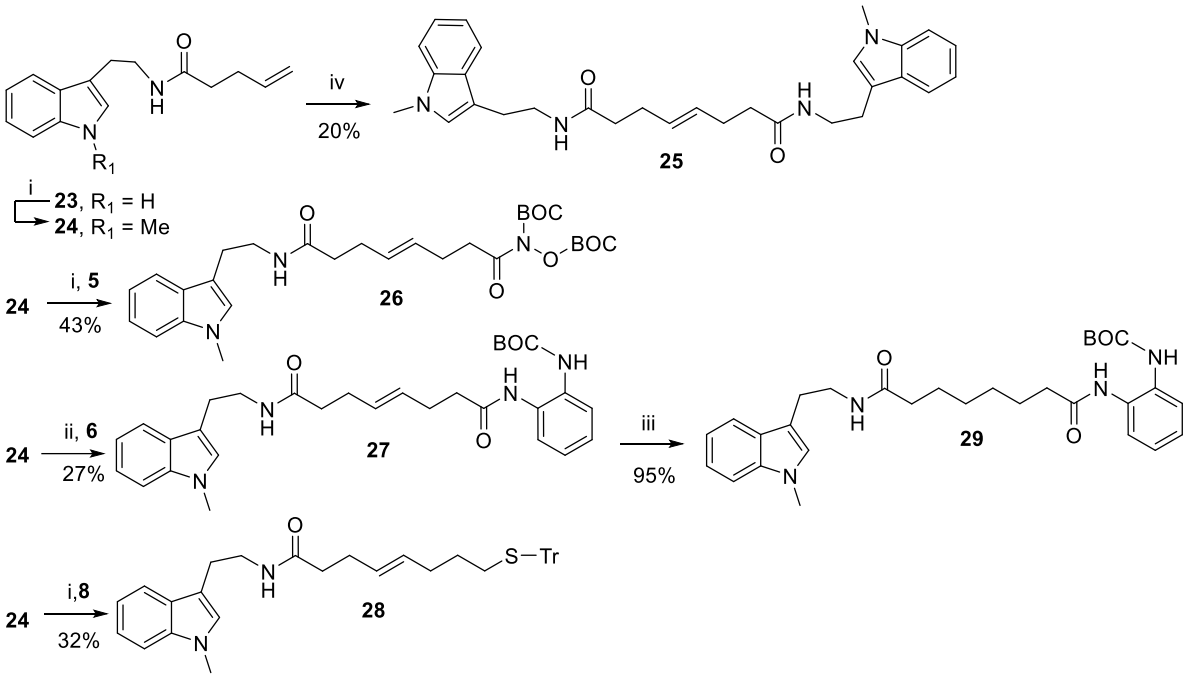

a: i) CH_3I, NaH, THF. i) Grubbs 1st generation catalyst, CH_2Cl_2, reflux. ii,iv) Grubbs 2nd generation catalyst, CH_2Cl_2, reflux. iii) H_2, Pd/C, AcOEt.

Syntheses

Reactions were monitored by thin layer chromatography when applicable with 0.25 mm silica gel plates (60F-254. E. Merck) and revealed with phosphomolybdic acid 5% weight in ethanol. ^{1}H NMR spectra were recorded in 5 mm diameter tubes with a Bruker spectrometer (^{1}H 400 MHz. ^{13}C 100 MHz), in $CDCl_3$. acetone D6 or DMSO D6 (for compound **2**) at 25 °C. The chemical shift scale expressed in ppm was calibrated on the basis of the deuterated solvent or tetramethylsilane as reference. High resolution mass spectra were recorded on a Waters Micro-TOF-Q and Q-2.

Pent-4-en-1-yl(trityl)sulfane **8**. To a solution of tritylthiol (19.49g, 70.5 mmol) and bromide (10.51g, 70.5mmol) in ACN (350 mL) was added K_2CO_3 (73.1g, 7.5 eq.). After stirring overnight at room temperature the solution was diluted with water (200 mL) and extracted (Et_2O, 3*200 mL). The combined organic layers were dried ($MgSO_4$) and concentrated under vacuum. Purification (Flash chromatography silica gel PE:EA 98:2) gave the expected compound **8** as a yellow oil (23g, 92%).^{1}H NMR ($CDCl_3$) δ ppm: 1.49 (m, 2H), 2.03 (m, 2H), 2.18 (t, 2H, J=7.33Hz), 4.94 (m, 2H), 5.67 (m, 1H), 7.22 (m, 3H), 7.30 (m, 6H), 7.44 (m, 6H). ^{13}C NMR ($CDCl_3$) δ ppm: 27.9, 31.4, 33.0, 66.5, 115.0, 126.5, 127.8, 129.6, 137.8, 145.0.

(Z/E)-1,8-bis(tritylthio)oct-4-ene **9**. Grubbs I catalyst (60mg) in DCM (3mL) was added over 6h (0.5mL/h rate) to a boiling solution of **8** (130mg, 0.38mmol) in DCM (3mL). The cool solution was then purified (Flash chromatography silica, PE/EA 100/0 (100mL), 95/5 (250mL), 90/10 (250mL), 85/15 (500mL)) and gave **9** (107mg, 86%) as a brown oil. ^{1}H NMR ($CDCl_3$) δ ppm: 1.30 (m, 2H), 1.79 (m, 2H), 2.02 (t, 2H, J=7.7Hz), 5.05 (m, 1H), 7.11 (m, 3H), 7.18 (m, 6H), 7.32 (m, 6H). ^{13}C NMR ($CDCl_3$) δ ppm: 27.4, 30.4, 30.7, 65.4, 125.5, 126.8, 126.9, 128.6, 144.0. HRMS Cald. for $C_{46}H_{44}NaS_2$: $[M+Na]^+$: 683.2777, Found:683.2809.

Methyl 1-(pent-4-en-1-yloxy)-2-naphthoate **12**. To a solution of phenol **11** (2g, 10 mmol) in DMF (10 mL) was added pentenylbromide (1.2 mL, 10 mmol), K_2CO_3 (1.34 g, 10mmol) and NaI (1.5 g, 10 mmol). After stirring overnight at ambient temperature the reaction is almost complete. NaI (10 mmol) was added and 12h more stirring gave total reaction. Saturated aqueous NaCl was added (100 mL) and the mixture extracted (Et_2O, 3x100 mL). The combined organic layers were dried ($MgSO_4$) and concentrated. Purification (Flash chromatography silica, PE/EA 100/0 (100mL), 95/5 (250mL), 90/10 (250mL), 85/15 (500mL)) gave the ether as a brown oil (2.4 g, 91%). ^{1}H NMR (400 MHz, $CDCl_3$) δ ppm: 2.06 (m, 2H), 2.35 (m, 2H), 3.96 (s, 3H), 4.12 (t, 2H, J=6.6Hz), 5.09 (m, 2H), 5.93 (m, 1H), 7.55 (m, 3H), 7.83 (m, 2H), 8.26 (m, 1H). ^{13}C NMR (100

MHz, $CDCl_3$) δ ppm : 18.1, 23.8, 29.6, 30.3, 33.7, 52.2, 75.8, 115.1, 119.3, 123.5, 123.7, 123.8, 126.4, 126.7, 126.9, 127.8, 128.3, 128.8, 136.7, 138.0, 157.3, 166.9.

Dimethyl 1,1'-(oct-4-ene-1,8-diylbis(oxy))(E)-bis(2-naphthoate) **13**. Grubbs catalyst (30mg) in DCM (3mL) was added over 6h (0.5mL/h rate) to a boiling solution of **12** (150mg, 0.55mmol) in DCM (3mL) and refluxed 1h more. The cool solution was then purified (flash chromatography silica PE/EA gradient 100/0 to 95/5 in 40 min, 90/10 in 10 min and 50/50 in 10min) to yield **13** (55mg, 39%) as an orange oil. ^{1}H NMR ($CDCl_3$) δ ppm: 2.05 (m, 4H), 2.34 (m, 4H), 3.96 (2s, 6H), 4.13 (t, 4H, J=6.4Hz), 5.60 (m, 2H), 7.58 (m, 6H), 7.85 (m, 4H), 8.29 (m, 2H). ^{13}C NMR ($CDCl_3$) δ ppm: 22.9, 29.2, 30.3, 33.7, 52.2, 75.9, 119.2, 123.7, 123.8, 126.6, 127.8, 128.3, 128.8, 29.7, 130.2, 136.7, 157.4, 166.9. HRMS Cald. for $C_{32}H_{32}NaO_6$ $[M+Na]^+$: 535.2091, Found: 535.2105.

(Z/E)-methyl 1-((8-((2-((tert-butoxycarbonyl)amino)phenyl)amino)-8-oxooct-4-en-1-yl)oxy)-2-naphthoate **15**. Prepared as **14** from **6** (92mg, 0.34mmol) and **12** (100mg, 0.34mmol) in DCM (3mL) and Grubbs II (50mg) in DCM (3mL). Purification (flash chromatography silica, PE/EA 100/0 to 85/15 over 60 min) gave **15** (65mg, 36%) as an orange oil. ^{1}H NMR ($CDCl_3$) δ ppm: 0.87 (m, 4H), 1.30 (m, 2H), 1.50 (3s, 9H), 1.65 (s large, 1H), 2.46 (2s, 2H), 3.95 (s, 3H), 4.12 (m, 2H), 6.97 (s large, 1H), 7.13 (m, 2H), 7.41 (m, 2H), 7.58 (m, 3H), 7.84 (dd, 2H, J=7.2, 8.7Hz), 8.11 (s large, 1H), 8.26 (dd, 1H). HRMS Cald. for $C_{31}H_{36}N_2NaO_6$ $[M+Na]^+$: 555.2466, Found: 555.2555.

Methyl 1-((8-((2-((tert-butoxycarbonyl)amino)phenyl)amino)-8-oxooctyl)oxy)-2-naphthoate **19**. Prepared as **17** from **15** (62mg, 0.12mmol) in EA (2mL) and Pd/C 10% (40mg). After dilution with DCM filtration gave **19** (57mg, 93%) as an orange oil directly used for next step. HRMS Cald. for $C_{31}H_{38}N_2NaO_6$ $[M+Na]^+$: 557.2622, Found: 557.2563.

Methyl 1-((8-((2-aminophenyl)amino)-8-oxooctyl)oxy)-2-naphthoate **20**. TFA (0.5mL, 6mmol) was added to a solution of **19** (57mg, 0.11mmol) in DCM (1.5mL) and the solution stirred for 3h. After dilution with EA, the solution was washed (3x5mL saturated aqueous NaCl). The combined aqueous extracts were neutralized to pH 7 (saturated aqueous $NaHCO_3$) and extracted (3x20mL, EA). The combined organic layers were dried ($MgSO_4$) and the solvents removed under vacuum. Purification (flash chromatography silica, PE/EA 100:0, 90:10, 82:18, 75:25, 50:50, 30:70, 0:100 100 mL each) gave **20** (38mg, 83%) as a yellow solid. ^{1}H NMR (400 MHz, Acetone D6) δ ppm: 1.49 (m, 4H), 1.63 (m, 2H), 1.77 (m, 2H), 1.97 (p, 2H, J=7.40Hz), 2.45 (t, 2H, J=7.30 Hz), 4.16 (t, 2H, J=7.40Hz), 4.55 (sb, 2H), 6.62 (td, 1H, J=1.44, 7.72Hz), 6.81 (dd, 1H, J=1.32, 7.96Hz), 6.94 (td, 1H, J=1.44, 7.96 Hz), 7.22 (dd, 1H, J=1.32, 7.84 Hz), 7.60 (m, 2H), 7.72 (d, 1H, J=8.64Hz), 7.82 (d, 1H, J=8.64Hz), 7.97 (m, 1H), 8.31 (m, 1H), 8.60 (sb, 1H).. ^{13}C NMR (100 MHz, Acetone D6) δ ppm: 171.2, 166.4, 156.9, 142.1, 136.6, 128.7, 128.3, 127.9, 126.6, 126.5, 125.9, 125.1, 124.7, 123.5, 123.4, 123.2, 119.7, 117.2, 116.8, 76.0, 51.5, 36.2, 30.2, 29.1 (x2 at 29.1 & 29.09 by DEPT135 and H-C correlation), 25.8, 25.6. HRMS Cald. for $C_{26}H_{30}N_2NaO_4$ $[M+Na]^+$: 457.2098, Found: 457.2094.

(Z/E)-methyl 1-((8-(tritylthio)oct-4-en-1(yl)oxy)-2-naphthoate **16**. Prepared as **12** from **11** (270mg, 1mmol), **14** (688mg, 2mmol) in DCM (9mL) and Grubbs I (150mg) in DCM (4.5mL) added at 0.8mL/h. After dilution with DCM purification (flash chromatography silica, PE/EA/TEA: 99.5/0/0.5, 250mL, 97/2.5/0.5, 500mL) gave **25** (294mg, 50%) as an orange oil. ^{1}H NMR ($CDCl_3$) δ ppm: 1.55 (p, 2H), 2.06 (m, 4H), 2.23 (m, 2H), 2.32 (q, 2H), 4.04 (2s, 3H), 4.18 (m, 2H), 5.45 (m, 2H), 7.28 (m, 3H), 7.35 (m, 6H), 7.49 (m, 6H), 7.66 (m, 3H), 7.93 (td, 2H, J=6.3, 6.8Hz), 8.35 (dd, 1H, J=7.0, 7.2Hz). ^{13}C NMR ($CDCl_3$) δ ppm: 22.4, 22.7, 23.8, 26.7, 28.5, 28.7, 29.1, 30.3, 30.4, 31.5, 31.6, 31.8, 52.2, 60.4, 66.5, 66.5, 75.9, 76.0, 77.3, 119.2, 119.3, 123.4, 123.7, 126.4, 126.5, 126.8, 127.6, 128.3, 128.8, 129.5, 129.6, 130.0, 130.1, 136.7, 145.0, 145.1, 157.4, 166.9, 166.9. HRMS Cald. for $C_{39}H_{38}NaO_3S$ $[M+Na]^+$: 609.2434, Found: 609.2420.

Methyl 1-((8-(tritylthio)octyl)oxy)-2-naphthoate **21**. Prepared as **17** from **16** (280mg, 0.48mmol) in EA (5mL) and Pd/C 10% (150mg). Filtration of the resulting solution gave **21** (235mg, 84%) as an orange oil. ^{1}H NMR ($CDCl_3$) δ ppm: 1.34 (m, 4H), 1.43 (m, 2H), 1.53 (m, 2H), 1.93 (m, 2H), 2.16 (t, 2H, J=7.2Hz), 3.98 (s,3H), 4.11 (t, 2H, J=7.2Hz), 7.22 (m, 3H), 7.3 (m, 6H), 7.45 (m, 6H), 7.6 (m, 3H), 7.87 (m, 2H), 8.28 (dd, 1H, J=Hz). ^{13}C NMR ($CDCl_3$) δ ppm: 28.5, 28.7, 29.1, 30.4, 31.6, 31.8, 52.2, 60.4, 66.5, 76.0, 119.2, 123.4, 123.7, 126.5, 126.8, 127.6, 128.3, 128.8, 129.6, 130.1, 136.7, 145.1, 157.4, 166.9. HRMS Cald. for $C_{39}H_{40}NaO_3S$ $[M+Na]^+$: 611.2590, Found: 611.2427.

Methyl 1-((8-mercaptooctyl)oxy)-2-naphthoate **22**. To a solution of tritylthiol **21** (136 mg, 0.23 mmol) in DCM (1.5 mL) was added at 0°C TFA (1.5 mL) and TES (0.15 mL). The solution was stirred 3h at room temperature, diluted with DCM (5mL), and washed with H_2O (2*20 mL). The resulting organic layer was dried ($MgSO_4$) and concentrated under vacuum. The crude oil was purified (Flash chromatography silica gel EA:PE 0:100, 100 mL, 2:98 250mL, 5:95 250 mL, 10:90 250 mL and 20:80 to finish) to yield **22** as a colourless oil (59.5 mg, 74.7%) with traces of disulphide, also isolated. ^{1}H NMR (400 MHz, $CDCl_3$) δ ppm: 1.40 (m, 6H), 1.60 (m, 4H), 1.97 (p, 2H, J=6.72Hz), 2.55 (q, 2H, J=7.53Hz), 3.99 (s, 3H), 4.13 (t, 2H, J=6.68Hz), 7.6 (m, 3H), 7.86 (dd, 1H, J=1.72,7 .44Hz), 7.88 (d, 1H, J=8.68Hz), 8.28 (d, 1H, J=1.4,7.92Hz). ^{13}C NMR (100 MHz, $CDCl_3$) δ ppm:. HRMS Cald. for $C_{20}H_{26}NaO_3S$ $[M+Na]^+$: 369.1495, Found: 369.1768.

(Z/E)-N1,N8-bis(2-(1-methyl-1H-indol-3-yl)ethyl)oct-4-ene-1,8-diamine **25**. Prepared as **13** from **24** (75mg, 0.30mmol) in DCM (3mL) and Grubbs I (20mg) in DCM (3mL). Purification (flash chromatography silica, PE/EA 100/0 to 85/15 over 30min, then to 0/100 over 20min) gave **25** (15mg, 20%) as a brown oil. ^{1}H NMR ($CDCl_3$) δ ppm: 2.11 (m, 2H), 2.23 (m, 2H), 2.95 (m, 2H), 3.56 (q, 2H, J=6.5Hz), 3.76 (s, 3H), 5.35 (m, 1H), 5.50 (m, 1H), 6.88 (s, 1H), 7.12 (t, 1H, J=7.0Hz), 7.23 (m, 2H), 7.31 (d, 1H, J=7.85Hz). ^{13}C NMR ($CDCl_3$) δ ppm: 25.3, 28.4, 32.7, 36.4, 39.8, 109.3, 111.6, 118.9, 119.0, 121.8, 126.8, 127.8, 129.8, 137.1, 172.3. HRMS Cald. for $C_{30}H_{36}N_4NaO_2$ [M+Na]+: 507.2730, Found: 507.2713.

(Z/E)-tert-butyl (tert-butoxycarbonyl)oxy(8-((2-(1-methyl-1H-indol-3-yl)ethyl)amino)-8-oxooct-4-enoyl)carbamate **26**. Prepared as **14** from **24** (106mg, 0.41mmol) and **5** (258mg, 0.82mmol) in DCM (3mL) with Grubbs I (50mg) in DCM (3mL). Purification (flash chromatography silica, PE/EA/TEA 99.5/0/0.5 250, 50/49.5/0.5 1L, 0/99.5/0.5 500mL followed by preparative TLC PE/EA 85/15 once and 50/50 twice) gave **26** (96, 43%) as a brown oil. ^{1}H NMR ($CDCl_3$) δ ppm: 1.52 (3s, 18H), 1.64 (s large, 1H), 2.15 (m, 2H), 2.29 (m, 2H), 2.36 (m, 2H), 2.88 (m, 2H), 2.95 (t, 2H J=6.8Hz), 3.58 (q, 2H, J=6.5Hz), 3.76 (2s, 3H), 5.50 (4m, 2H), 6.90 (s, 1H), 7.11 (td, 1H, J=7.9Hz), 7.23 (m, 1H), 7.30 (2s, 1H), 7.60 (d, 1H, J=7.9Hz). HRMS Cald. for $C_{29}H_{41}N_3NaO_7$ $[M+Na]^+$: 566.2837, Found: 566.2969.

(E/Z)-tert-butyl (2-(8-((2-(1-methyl-1H-indol-3-yl)ethyl)amino)-8-oxooct-4-enamido)phenyl)carbamate **27**. Prepared as **26** from **25** (77mg, 0.3mmol) and **6** (89mg, 0.3mmol) in DCM (3mL) with Grubbs II (40mg) in DCM (3mL). Purification (flash chromatography silica, PE/EA 100/0 to 95/5 over 15min, to 85/15 over 15min, to 0/100 over 30min) gave **27** (41mg, 27%) as an orange oil. ^{1}H NMR ($CDCl_3$) δ ppm: 1.52 (2s, 9H), 1.61 (m, 4H), 2.15 (m, 2H), 2.38 (m, 2H), 2.91 (m, 2H), 3.50 (q, 2H, J=6.3Hz), 3.76 (3s, 3H), 5.49 (m, 1H), 5.50 (s large, 1H), 5.58 (m, 1H), 6.86 (3s, 1H), 7.14 (m, 3H), 7.28 (m, 2H), 7.44 (2m, 1H), 7.58 (m, 1H), 8.08 (s broad,1H), 8.48 (s broad,1H). HRMS Cald. for $C_{30}H_{38}N_4NaO_4$ $[M+Na]^+$: 541.2785, Found: 541.2773.

(E)-N-(2-(1-methyl-1H-indol-3-yl)ethyl)-8-(tritylthio)oct-4-enamide **28**. Prepared as **26** from **25** (120mg, 0.5mmol) and **8** (344mg, 1mmol) in DCM (9mL) with Grubbs I (150mg) in DCM (7mL) at 1.2mL/h flow rate. Purification (flash chromatography silica, PE/EA/TEA 99.5/0/0.5 250mL, 50/49.5/0.5 1L, 0/99.5/0.5 500mL followed by preparative TLC PE/EA 50:50 once and 65:35 twice) gave **28** (91mg, 32%) as a brown oil. ^{1}H NMR ($CDCl_3$) δ ppm: 1.27 (s, 1H), 1.40 (p, 2H, J=7.3Hz), 1.88 (q, 2H), 2.11 (td, 4H), 2.23 (q, 2H), 2.95 (t, 2H, J=6.7Hz), 3.57 (q, 2H, J=6.6Hz), 3.75 (s, 3H), 5.25 (m, 2H), 6.68 (s, 1H), 7.12 (m, 1H), 7.20 (m, 3H), 7.28 (m, 8H), 7.41 (m, 6H), 7.59 (d, 1H, J=7.9Hz). ^{13}C NMR ($CDCl_3$) δ ppm: 25.3, 28.3, 28.5, 31.4, 31.7, 32.7, 36.7, 39.8, 66.4, 77.2, 109.3, 111.6, 118.9, 119.0, 121.8, 126.5, 126.8, 127.8, 129.3, 129.6, 130.4, 137.1, 145.0, 172.3. HRMS Cald. for $C_{38}H_{40}N_2NaOS$ $[M+Na]^+$: 595.2754, Found: 595.2754.

tert-butyl (2-(8-((2-(1-methyl-1H-indol-3-yl)ethyl)amino)-8-oxooctanamido)phenyl)carbamate **29**. Prepared as **17** from **27** (40mg, 0.08mmol) in EA (1mL) and Pd/C 10% (25mg). The resulting solution was diluted with DCM and filtered to give **29** (38mg, 95%) as an orange oil. ^{1}H NMR ($CDCl_3$) δ ppm: 1.37 (m, 2H), 1.53 (s, 9H), 1.63 (m, 2H), 1.72 (m, 6H), 2.12 (t, 2H, J=7.4Hz), 2.37 (t, 2H, J=7.4Hz), 2.96 (t, 2H, J=6.8Hz), 3.58 (q, 2H, J=6.6Hz), 3.77 (2s, 3H), 5.64 (s large, 1H), 6.89 (2s, 1H), 7.05 (s large, 1H), 7.15 (m, 3H), 7.27 (m, 2H), 7.46 (2m, 2H), 7.60 (m, 1H), 8.24 (s large, 1H). HRMS Cald. for $C_{30}H_{40}N_4NaO_4$ $[M+Na]^+$: 543.2942, Found: 543.2779.

Table S1. Summary of current and previous CM results

Isolated yields are given with Grubbs catalyst used in parentheses (I) for Grubbs 1rst generation and (ii) for 2nd generation.

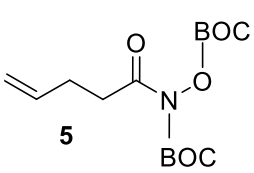

5

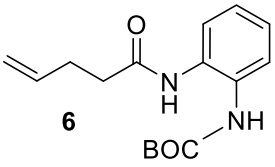

6

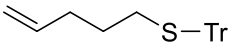

8

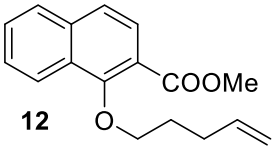

12

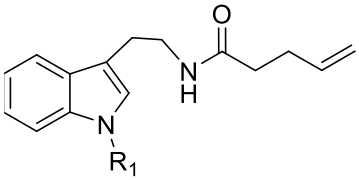

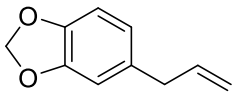

30

23, R_1 = H
24, R_1 = Me

	8	5	6	12	23	24	30
8	86 (I)			50 (I)		32 (I)	
5		70 (I)		48 (I)		43 (I)	59 (I)
6			72 (II)	36 (II)		27 (II)	
12				39 (I)			
23					0		
24						20 (II)	
30							

^{1}H and ^{13}C NMR spectra

^{1}H NMR **18** (DMSO D_6)

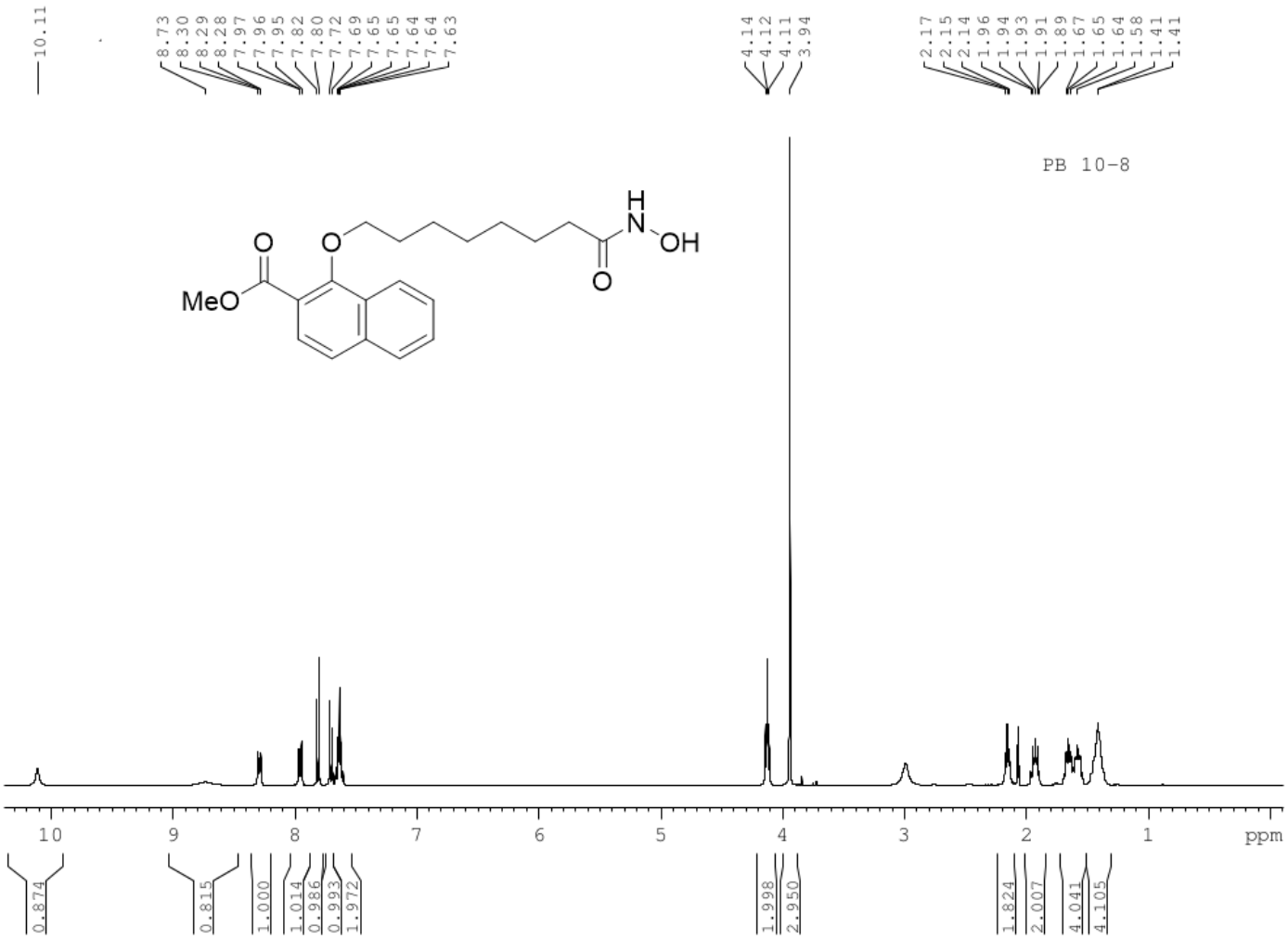

^{13}C NMR **18** (DMSO D_6)

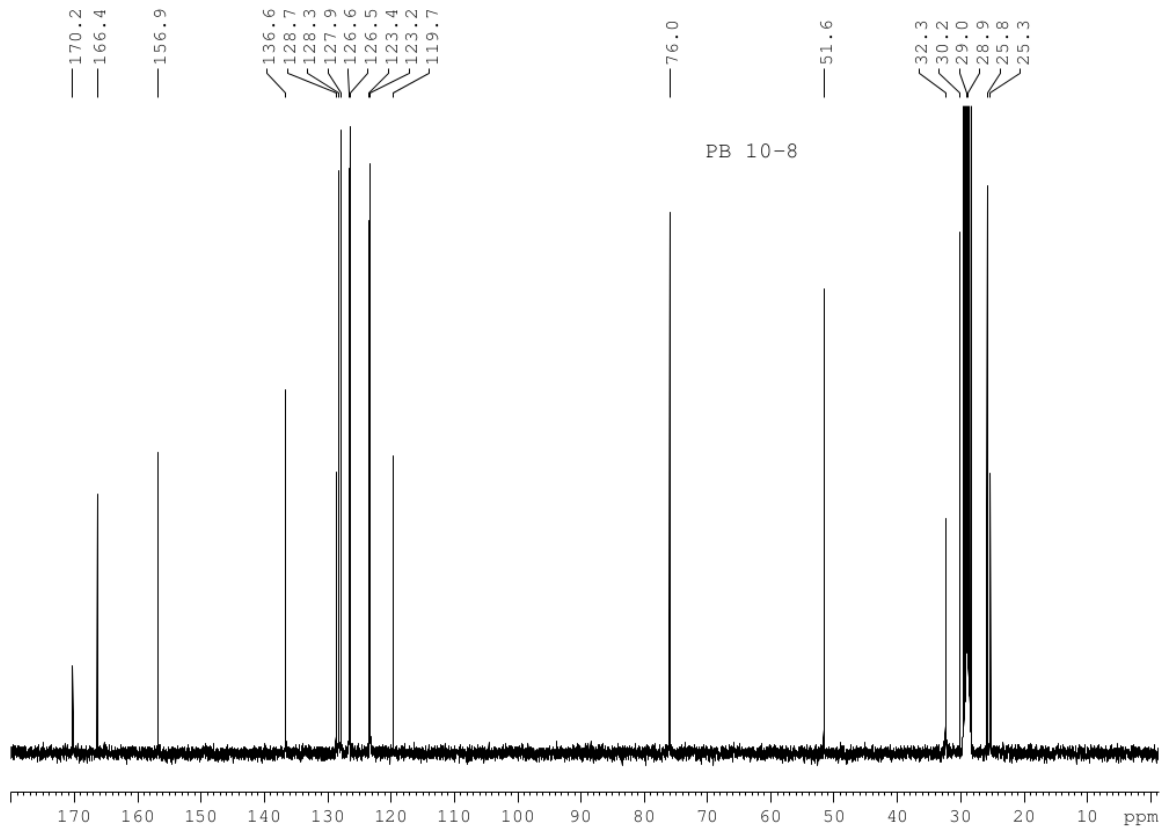

^{1}H NMR **20** (Acetone D_6)

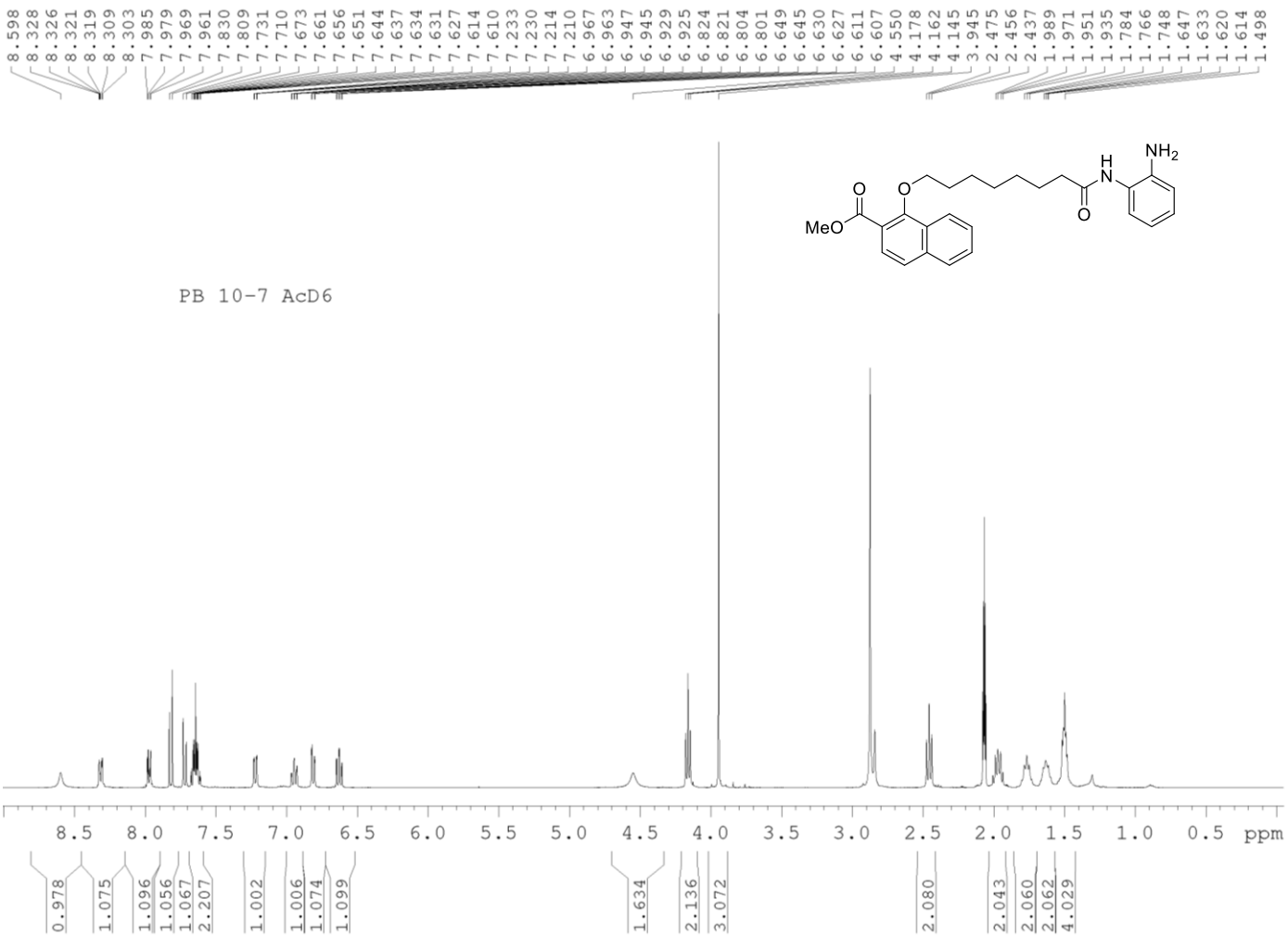

^{13}C NMR **20** (Acetone D_6)

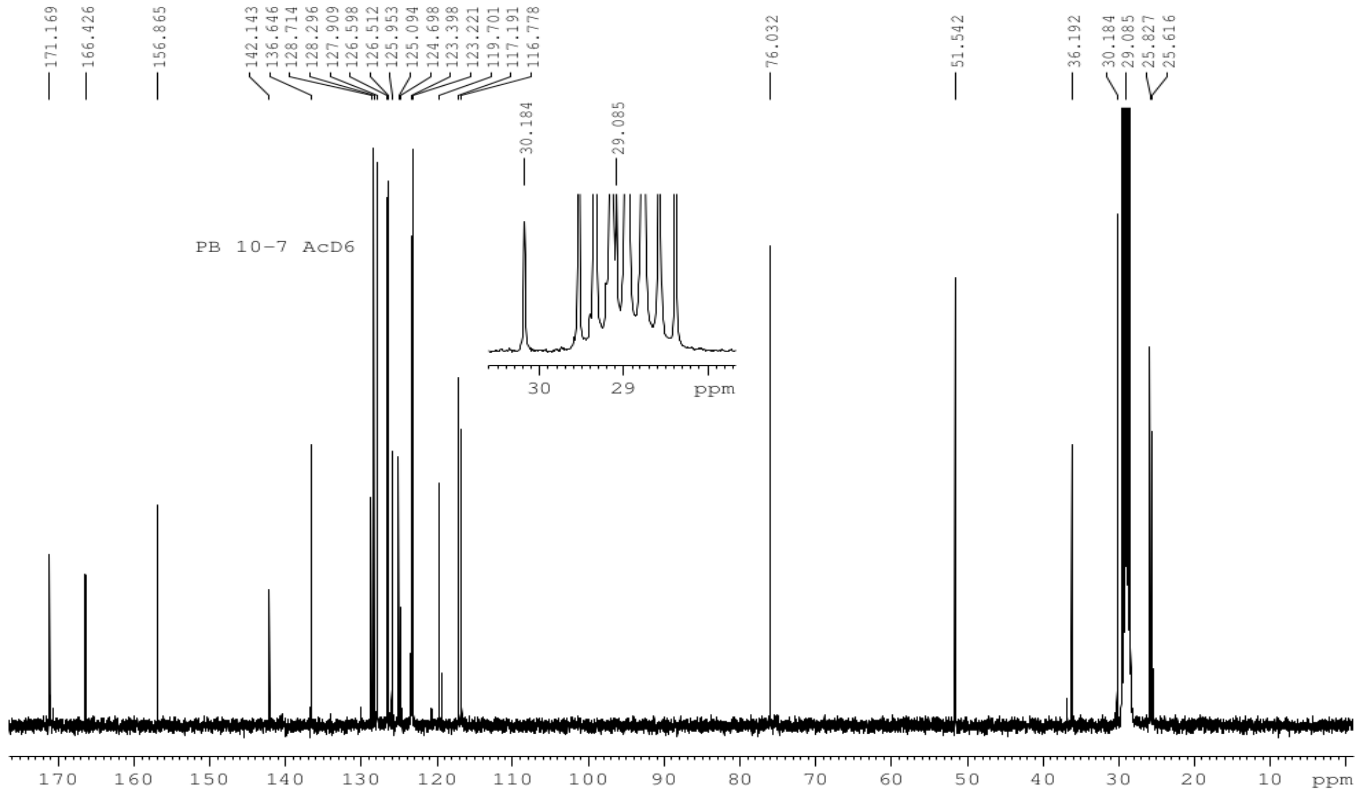

^{1}H NMR **22** ($CDCl_3$)

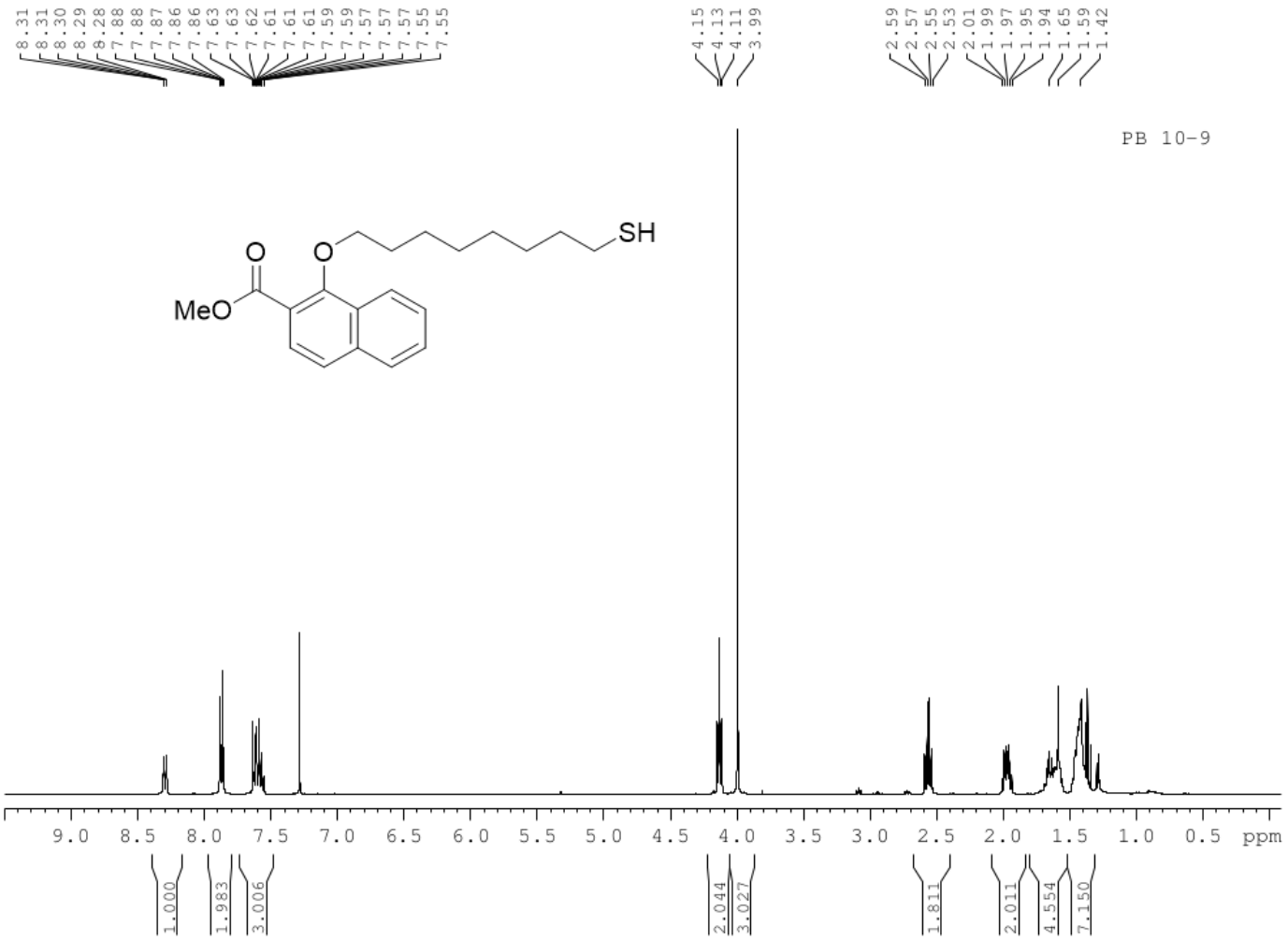

^{13}C NMR **22** ($CDCl_3$)

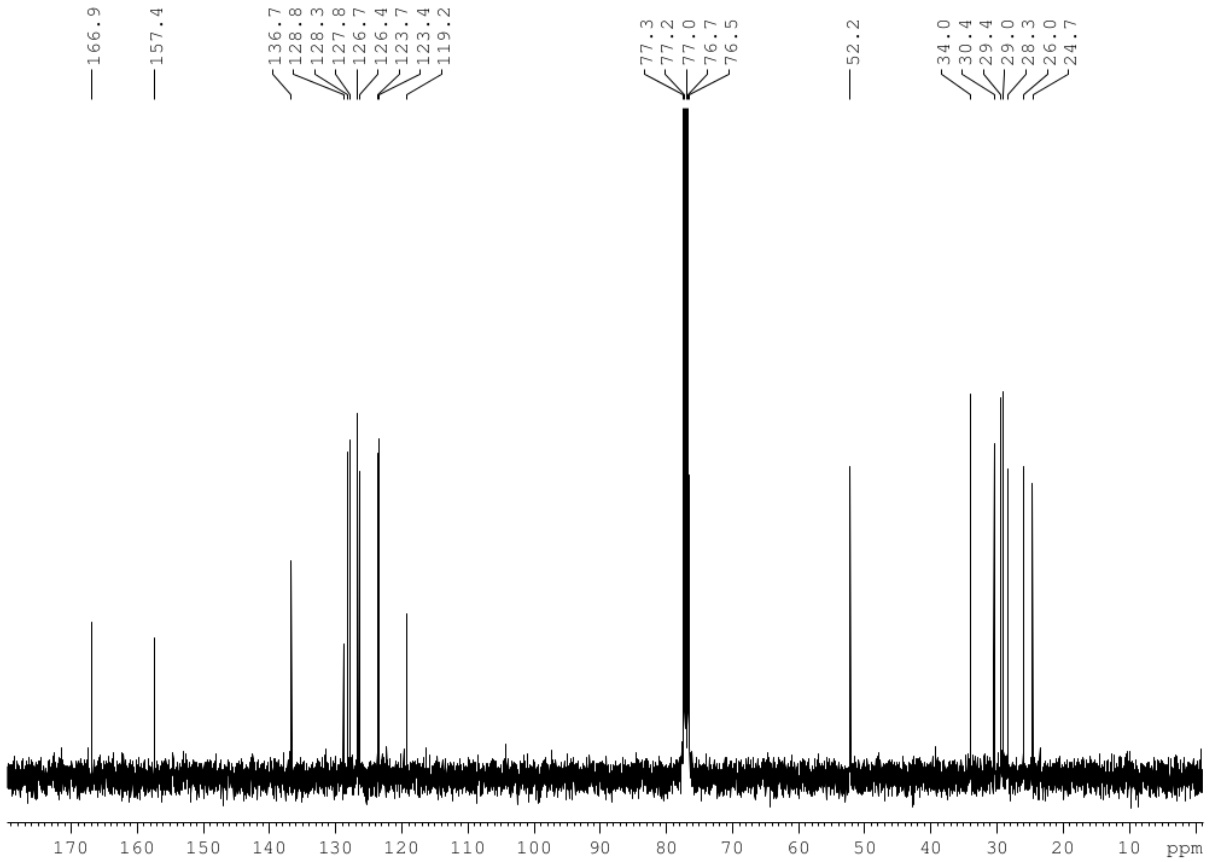

HPLC chromatograms

HPLC for compounds **18**, **20** and **22** were performed on Hitachi equipped with an auto-sampler, a diode array detection DAD L-2455. 1 µL of MeOH solution of compound at 1-4mg/2mL concentrations was injected. Two methods were used to assess the compound purity >= 95%. The purity is in brackets after compound number.

Method A with Column Phenomenex POLAR-RP (4 µm. 4.6 x 150mm)

Compound **18 (100%)**: Eluting system ACN:H_2O 1/1 v/v flow 0.25 mL/min.

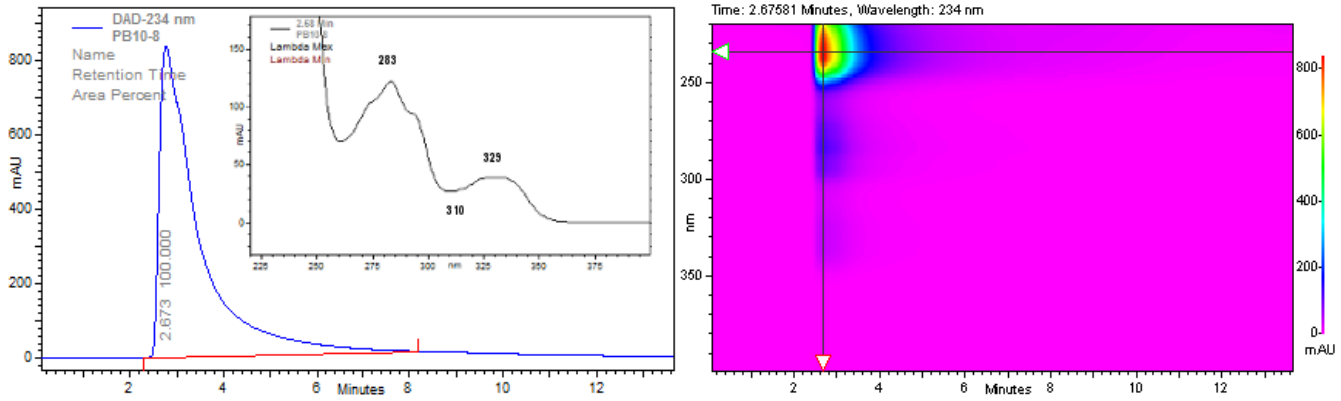

Compound **20 (97%)**: Eluting system ACN:iPrOH 1/1 v/v flow 0.25 mL/min.

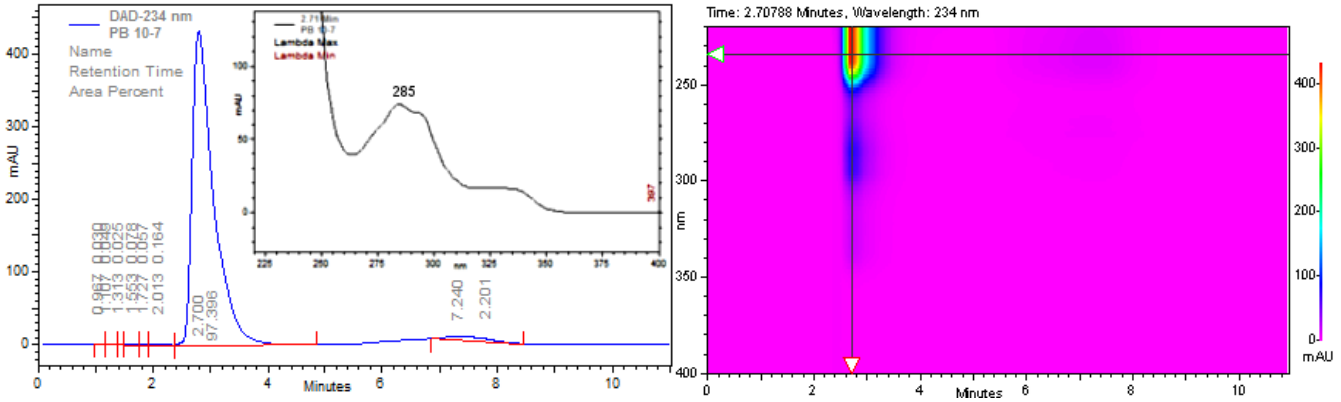

Compound **22 (98%)**: Eluting system ACN 100%, flow 0.5 mL/min. Column

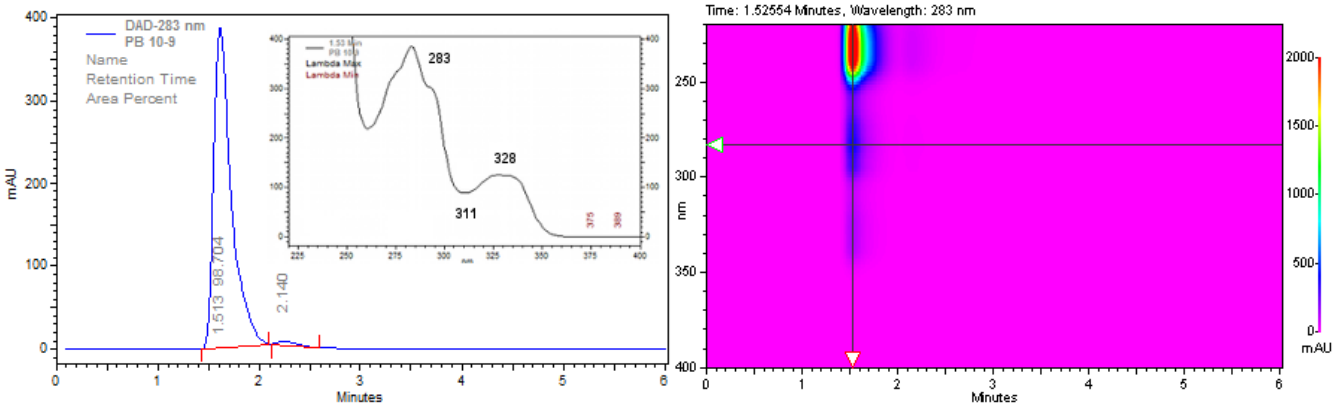

Method B with Phenomenex POLAR-RP (4 µm. 4.6 x 150mm)

Compound **18 (96%)**: Eluting system ACN:H_2O 1/1 v/v flow 0.25 mL/min.

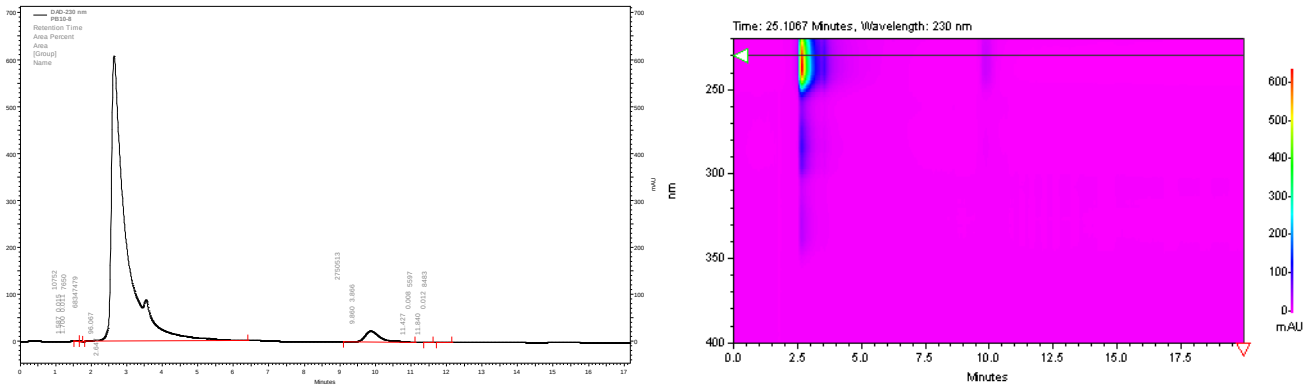

Compound **20 (95%)**: Eluting system ACN:iPrOH 1/1 v/v flow 0.25 mL/min.

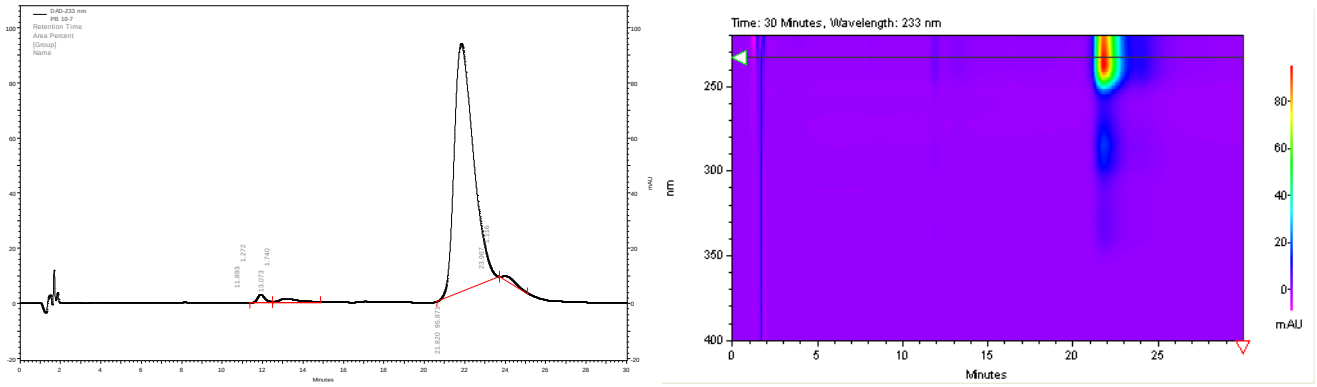

Compound **22 (95%)**: Eluting system ACN 100%, flow 1 mL/min.

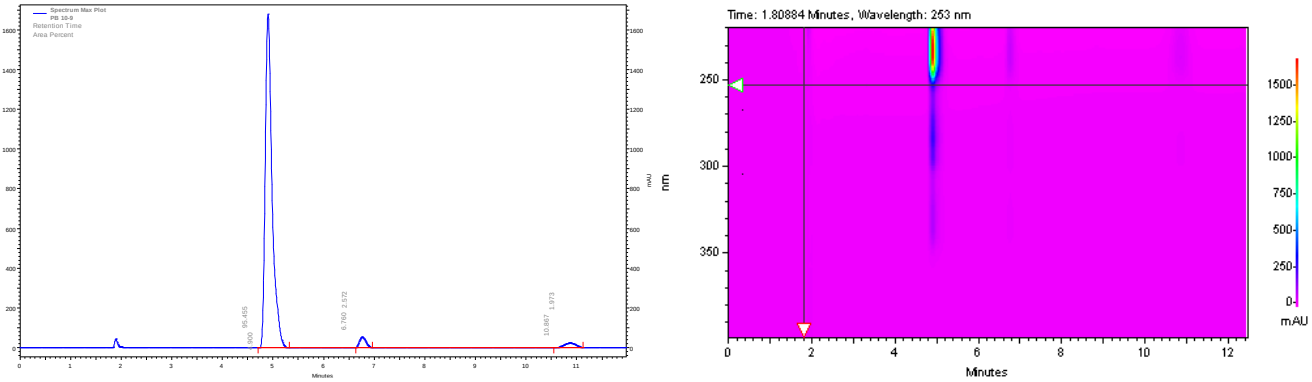

Biology

HDAC profiling

Compounds were tested in vitro for their inhibitory effect of HDACs (1 to 11) and sirtuins (1-3, 6) on lysine deacetylation on the platform at Cerep/Eurofins (Celle L'Evescault, France). Briefly, each recombinant HDAC was incubated with its fluorogenic acetylated substrate in presence or absence of the tested compound, and acetylation was further measured by fluorometry. Reference compounds include TSA for HDAC1-10, Scriptaid for HDAC11, suramin for sirtuin1-2, niacinamide for sirtuin3, EX-527 for sirtuin6.

Cell culture

The human pleural mesothelial cell line, MeT-5A and the human lung cancer cell line, A549 were obtained from ATCC. The mesothelioma, Meso13, Meso 163, and adenocarcinoma (ADCA) ADCA 72 cell lines were established from the pleural fluids of mesothelioma or lung ADCA patients, respectively. Cell lines were characterized by measuring mRNA expression of usual mesothelioma (P16, Podoplanin, keratin 5, Wilm's Tumor antigen-1 (WT-1) and calretinin) and lung ADCA (Thyroid Transcription Factor-1 (TTF-1), Epithelial cell adhesion molecule (EPCAM) and Carcinoembryonic Antigen Related Cell Adhesion Molecule 1 (CEACAM-1)) differential markers (Gueugnon et al., Am J of Pathol, 2011). All cell lines were maintained in RPMI medium (Invitrogen) supplemented with 2 mM L-glutamine, 100 IU/ml penicillin, 0.1 mg/ml Streptomycine and 10% heat inactivated fetal calf serum (FCS) (Eurobio).

BRET experiments.

Principle for the global HDAC inhibition in cells by BRET assay.

A bioluminescence resonance energy transfer is used in this assay, the luminescence being obtained directly in living cells transfected with a histone H3 tagged with a yellow fluorescent protein, the counterpart being a bromodomain tagged with *Renilla luciferase*, and coelenterazine is used as the reagent for luminescence activation.

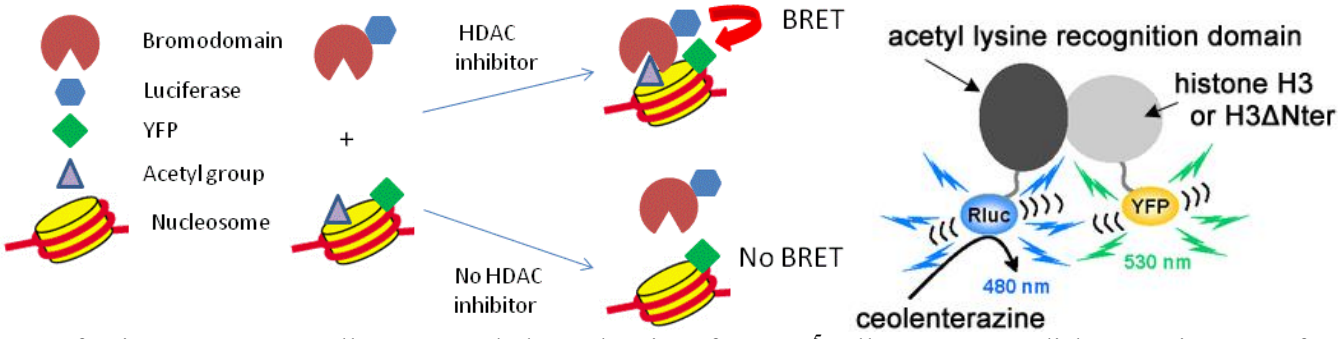

Transfections- MeT-5A cells were seeded at a density of $2.5x10^5$ cells per 35 mm dish. Transient transfections were performed 1 day later using Attractene (Qiagen), according to the manufacturer's protocol. MeT-5A cells were transfected with 0.6 µg Rluc-Brd cDNA and 1.2 µg YFP-fused histone H3 cDNA. One day after transfection, cells were transferred into 96-well microplates (microplate 96 well, white, Berthold Technologies) at a density of $3x10^4$ cells per dish. After 8h, cells were treated with the different compounds. The following day, BRET measurements were performed as described below.

BRET measurements- All BRET measurements were performed at room temperature using the Mithras LB 940 microplate analyzer (Berthold Technologies). Cells were pre-incubated for 15 min in PBS in the presence of 2.5 µM coelenterazine, following with light-emission acquisition at 485 and 530 nm done five times. The BRET signal was expressed in milliBRET units (mBu). The BRET unit has been defined previously as the ratio of emission 530 nm/485 nm obtained when the two partners are present, corrected by the ratio 530 nm/485 nm obtained under the same experimental conditions, when only the partner fused to Renilla luciferase was present in the assay.

Cell viability and toxicity evaluation.

Cells were seeded in 96-well plates at a density of $5x10^3$ cells per well. After 24 h, cells were treated with increasing doses of HDACi for 72 h. Toxicity and viability were sequentially determined. Cell toxicity was measured using CellTox™ Green Cytotoxicity Assay (Promega) (measure of cell permeability), followed by cell viability evaluated using CellTiter-Glo® Luminescent Cell Viability Assay (measure of ATP).

RNA isolation and measure of gene expression

Cells were seeded in 6-well plates at a density of $2x10^5$ cells per well. After 24 h, cells were treated with HDACi for 24 h. Total RNA was isolated using the Nucleospin® RNAII Kit according to the manufacturer's protocol (Macherey-Nagel). One microgram of total RNA was reverse-transcribed using Moloney murine leukemia virus reverse transcriptase (Invitrogen). Real-time PCR (qPCR) was carried out using an Mx3500P thermocycler (Stratagene). PCR reactions were performed using QuantiTect Primer Assays (Qiagen) and the RT² Real- Time SYBR-Green/ROX PCR Mastermix (Qiagen), according to the manufacturer's instructions. The relative amount of the target RNA, called the starting quantity (SQ), was determined using the Mx4000 software, by comparison with the corresponding standard curve for each sample performed in duplicate. Each transcript level was normalized by division with the expression values of the acidic ribosomal phosphoprotein P0 housekeeping gene (*RPLP0*), used as an internal standard.

Western blot analysis

Cells were seeded in 6-well plates at a density of $2x10^5$ cells per well. After 24 h, cells were treated with HDACi for 6 h or 20 h. Cells were washed with cold PBS and lysed with ice-cold RIPA buffer (Sigma-Aldrich) supplemented with protease inhibitor cocktail (Sigma-Aldrich). Cell lysates were transferred into 1.5 ml tubes. DNA was fragmented using sonication. After centrifugation at 13,000 g for 5 min at 4 °C, supernatant protein levels were determined using BCA kit according to the manufacturer's recommendations. 10 µg from each sample were electrophoresed through a 4-20 % polyacrylamide-SDS gel and transferred onto nitrocellulose membrane (Millipore). After blocking in PBS containing 0.2% Tween 20 (Sigma-Aldrich) (PBS-T) and 3% (w/v) bovine serum albumin (BSA) for 1 h at room temperature (RT), the membrane was incubated overnight at 4 °C with primary antibody diluted in blocking buffer. The membrane was washed three times with PBS-T and incubated for 1 h with secondary antibody conjugated to fluorophore diluted 1/1000 in blocking buffer. After three washes with PBS-T, analysis of the membrane was performed using a ChemiDoc™ MP Imaging System (Bio-Rad).

Antibody	Company	References	Used Concentration
Anti-Histone H3	Active Motif	39763	1 µg/ml
Anti-acetylated histone H3	Active Motif	39140	1 µg/ml
Anti-α tubulin	Abcam	ab4074	1 µg/ml
Anti-acetylated α tubulin	Abcam	ab24610	0.1 µg/ml
Alexa Fluor® 488 goat anti-mouse IgG	Molecular probes	A11029	1µg/ml
Alexa Fluor® 647 goat anti-rabbit IgG	Molecular probes	A21245	1µg/ml

Figure S1.

Characterisation of compounds' activities. MeT-5A cells were transfected with phRluc-C1-BrD and pEYFP-C1 histone H3 and treated for 24 h with increasing doses of the different compounds. Then, BRET signals were measured as described in the materials and methods section. A: Dose-dependent HDAC inhibition in cells determined by a BRET assay (n=2). B: Evaluation of possible interference of compound with BRET signal measurement (n=2). None of them presented intrinsic properties that could modify the measured BRET signal. C: Dose-dependent toxicities indicating that none of the compounds are toxic at the tested doses except compound 24 at 100µM (red arrow).

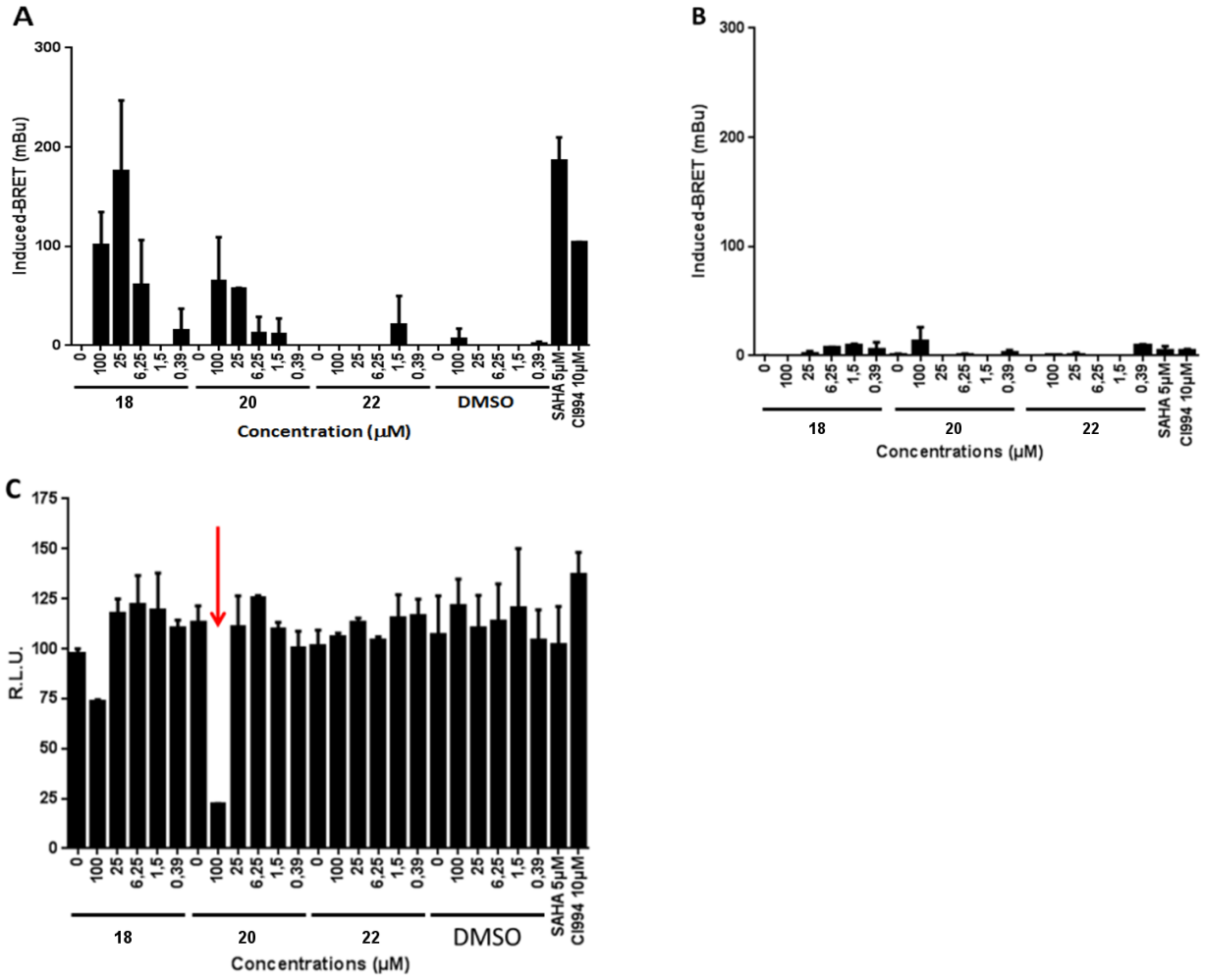

Figure S2.

Pharmacological characterization of drugs for their ability to lead to histone acetylation using BRET. MeT-5A cells were transfected with phRluc-C1-BrD and pEYFP-C1 histone H3 and treated for 24 h with increasing doses of the different compounds.

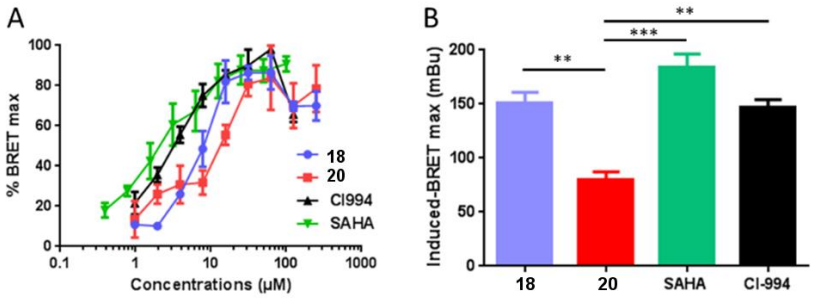

Then, BRET signals were measured as described in the materials and methods section. A) Dose response curves for the different drugs. 100% corresponds to the maximal induced BRET signal measured. B) HDACi-induced BRET max values measured for the different drugs. Results are the means ± SEM of three independent experiments. ** $p<0.01$; *** $p<0.01$.

Figure S3.

Pharmacological characterization of compound **18** toxicity on MPM and lung ADCA cells. Meso 163, Meso 13, ADCA 72 and A549 cells were treated with increasing doses of SAHA or of compound **18** for 72h. Then, viability (black curves) and toxicity (green curves) were determined. Results are means ± S.E.M. of three independent experiments.

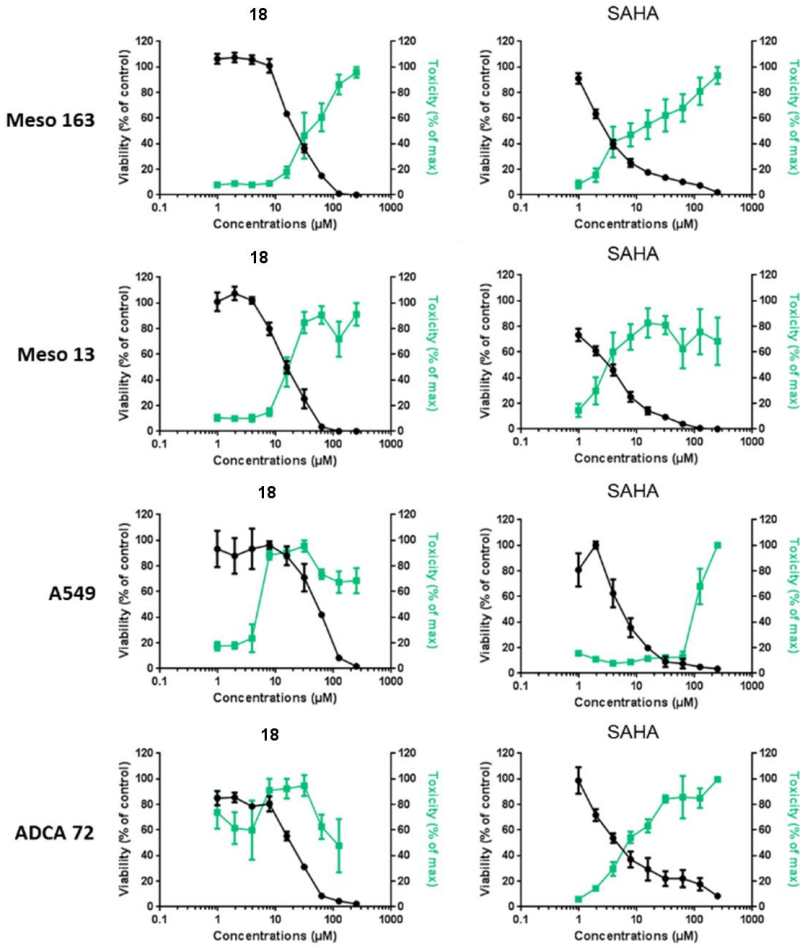

Figure S4.

Compound **18** inhibition of HDAC isoforms *in vitro*.

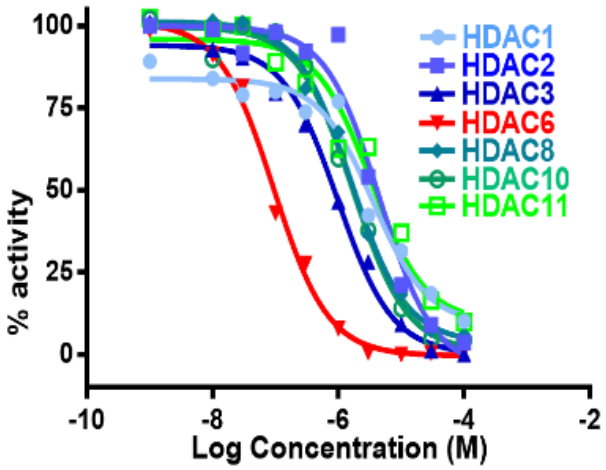

Figure S5.

Kinetic of BRET induction. MeT-5A cells were transfected with phRluc-C1-BrD and pEYFP-C1 histone H3 and treated for 6, 24, 26 or 48h with the different compounds.

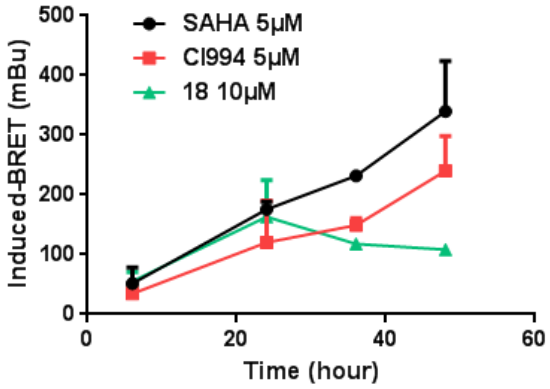

Molecular Docking

Crystal structures of HDAC isoforms (downloaded from Protein Data Bank: HDAC1 – 5ICN, HDAC2 – 4LXZ, HDAC3 – 4A69, HDAC4 - 4CBY, first catalytic domain of HDAC6- 5G0G, second catalytic domain of HDAC6 – 5EDU, HDAC7 – 3ZNR, HDAC8 – 1T64) and homology models of three HDAC isoforms (HDAC5, HDAC9 and HDAC11) from Professor Olaf Wiest group (http://www3.nd.edu/~owiest/) were used for virtual docking study of (*S*)-TSA and synthetized compound **18**.

Docking studies were performed with GOLD software 5.6.0, using ChemScore as the scoring function. The protein structures were prepared with PlayMolecule web server (https://playmolecule.org/). The binding cavity for *(S)*-TSA and **18** was set around Zn^{2+} ion in area within 15 Å. All torsion angles in TSA and compound **18** were allowed to rotate freely. The water molecules from the crystal structures were left in the active pocket to toggle and spin in order to examine their importance during ligand-protein recognition. For each ligand 30 docking runs were performed and tested several different docking setups in order to find the best concordance with the crystal structure of inhibitor (HDAC1, HDAC2, HDAC3, HDAC4, HDAC6, HDAC7, HDAC8 and HDAC10) complexes. The validity of homology and crystal structure models were confirmed by comparing experimentally observed binding modes of HDAC inhibitors and re-docked binding modes of the same inhibitors (calculation of RMSD values). We performed the geometrical optimization with *(S)*-TSA and compound **18** (Hartree-Fock method, 3-21 G basis set).

Table S2.

Inhibitory profile of *(S)*-TSA against zebrafish[i] and human HDAC6 as well as against human HDAC1−11 and calculated GOLD ChemScore Fitness Function calculated after docking of *(S)*-TSA and compound **18** into each HDAC isoform. The important interactions between compounds and amino acid residues are detailed, in bold for those common to *(S)*-TSA and **18**.

		(S)-TSA			***Compound 18***		
	Protein model	**IC_{50} (nM)**	**GOLD ChemScore**	**Important interactions with amino acid residues**	**GOLD ChemScore**	**IC_{50} (nM)**	**Important interactions with amino acid residues**
HDAC1	PDB: **5ICN**	206.30±15.84	29.6285	G149, F150, H178, F205, R270, L271	25.3775	3500	H140, H141, D176, H178 and L271
HDAC2	PDB: **4LXZ**	612.65±116.60	34.9495	G144, F155, H183, F210, L276, Y308	33.1958	3400	H145, H146, Y209, F210, G306 and Y308
HDAC3	PDB: **4A69**	320.80±27.01	30.1326	P23, G143, F144, H172, F200 and L266	25.7446	1000	P23, D93, F144, D170, Q255 and G296
HDAC4	PDB: **4CBY**	6341±627.91	33.2653	P676, H802, H803, F812, F871, P942 and L943	31.3067	n.a.	H802, H803, F871 and G974
HDAC5	Homology model	6325±117.38	25.5396	a	23.1221	n.a.	a
HDAC6 CDII	PDB: **5EDU**	11.1±0.62	35.9805	H610, G619, F620, C621, H651, F679, F680, L749 and E779	30.7607	95	H610, F680, M682 and Y782
HDAC6 CDI	PDB: 5G0G		40.0427	H193, F202, D230, W261, K330 and G361	34.5816		H82, P83, S150, H193 and G361 (H_2O-2095)
HDAC7	PDB: **3ZNR**	1823.50±6.36	31.6455	a	31.6097	n.a.	a
HDAC8	PDB: **1T64**	312.20±3.96	41.2816	H142, H143, F152, F208 and Y306	35.6581	1600	H142, P273 and Y306
HDAC9	Homology model	4824±228.40	31.8168	a	28.812	n.a.	a
HDAC10	PDB: **5TD7**	403.35±10.25	30.0848	A24, H136, H137, G145, F146, S203 and W205	26.5149	1600	A24, I27, H136, H137. W205 and E274
HDAC11	Homology model	2684.00±398.81	35.8161	H142, H143, F152, Y209, R267 and L268	31.3563	6600	G151, F152, I208 and Y304

a: Physical closure of the active site. In case of HDAC5, HDAC7 and HDAC9 enzymes none of predicted binding poses of **18** had shown metal-ligand coordination)

Figure S6.

(*S*)-TSA binding into the homology models of Class I (A-HDAC1, *B*-HDAC2, *C*-HDAC3 and *D*-HDAC8)

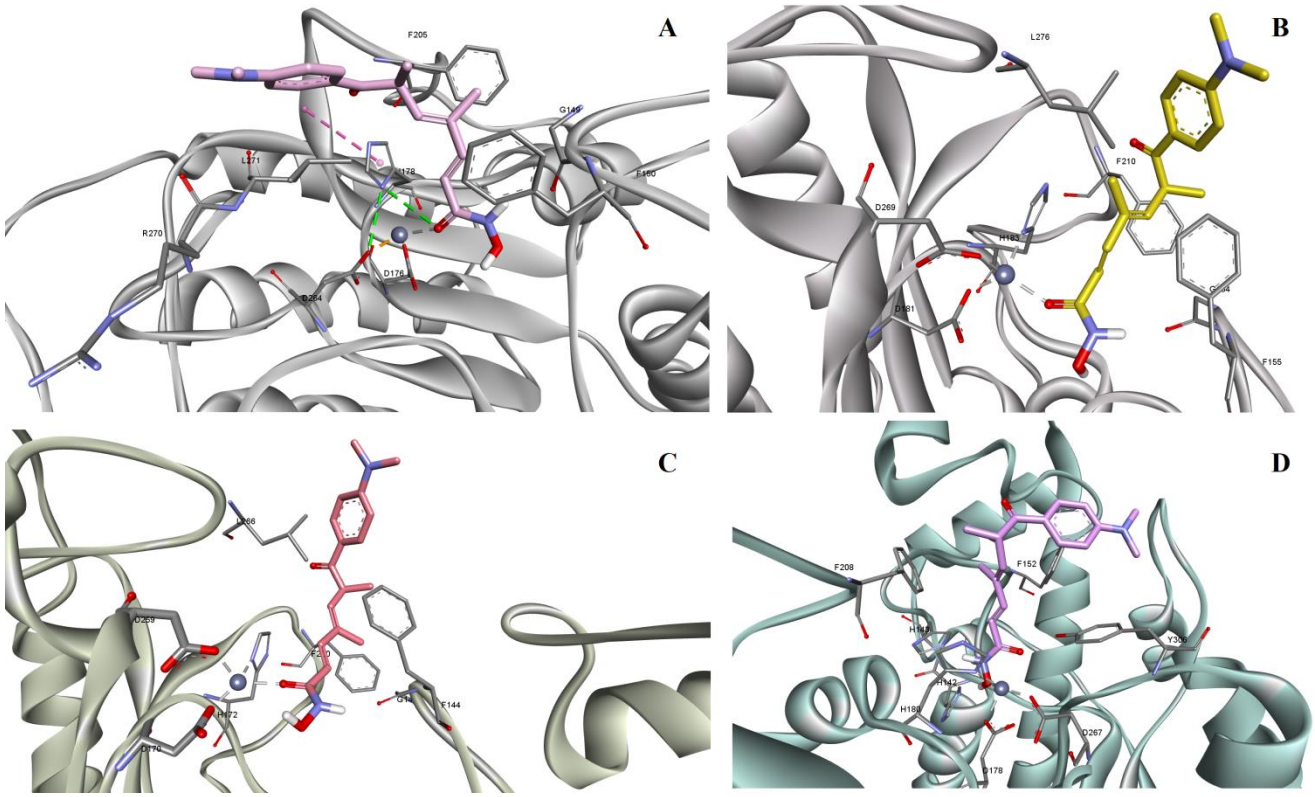

Figure S7

(*S*)-TSA binding into the homology models of Class IIa (*A*-HDAC4, *B*-HDAC5, *C*-HDAC7 and *D*-HDAC9)

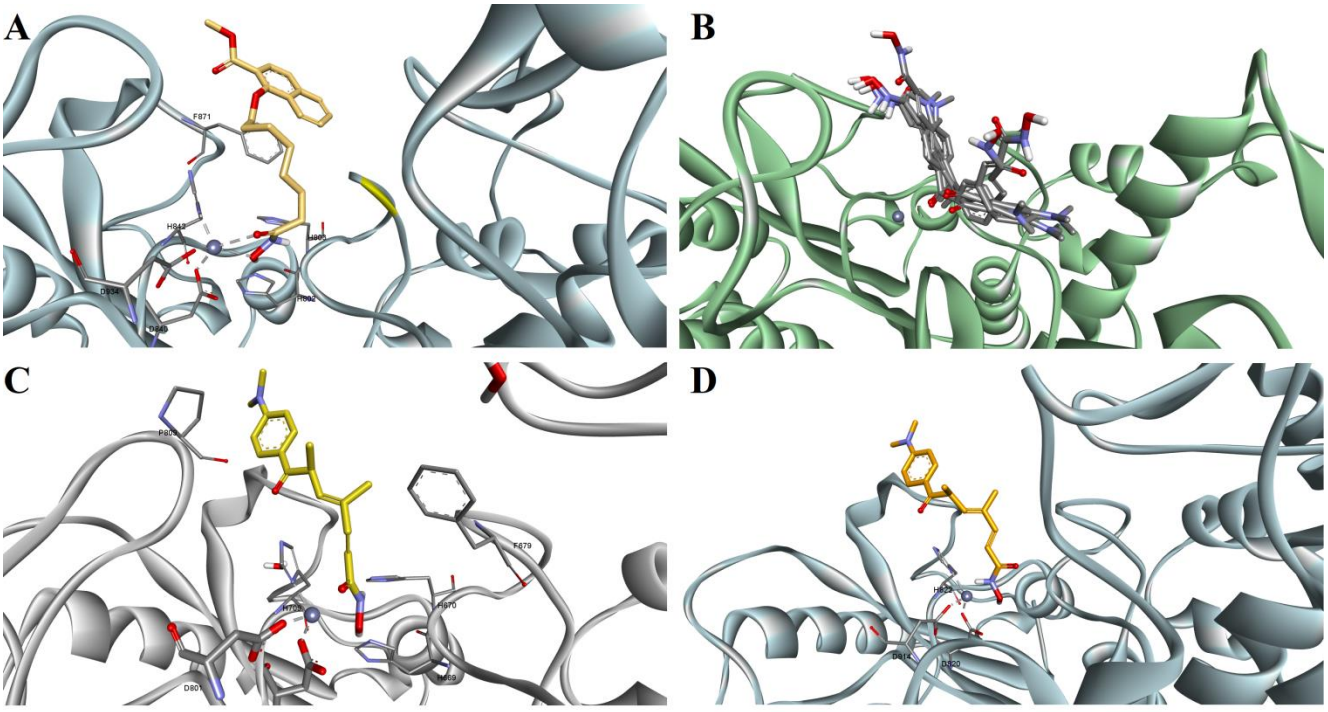

Figure S8

(*S*)-TSA binding into the homology models of Class IIb (*A*-HDAC6 (CD2) *B*-HDAC6 (CD1) and *C*-HDAC10)

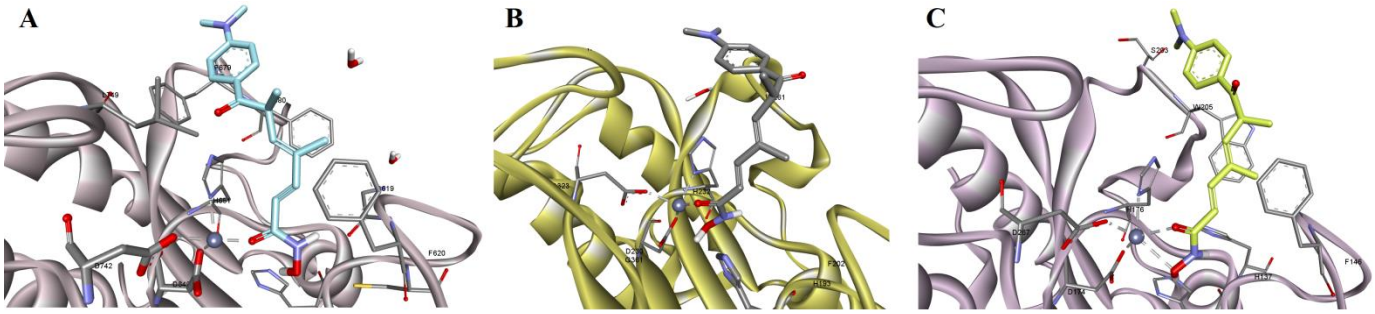

Figure S9

(*S*)-TSA binding into the homology models of Class IV (HDAC11)

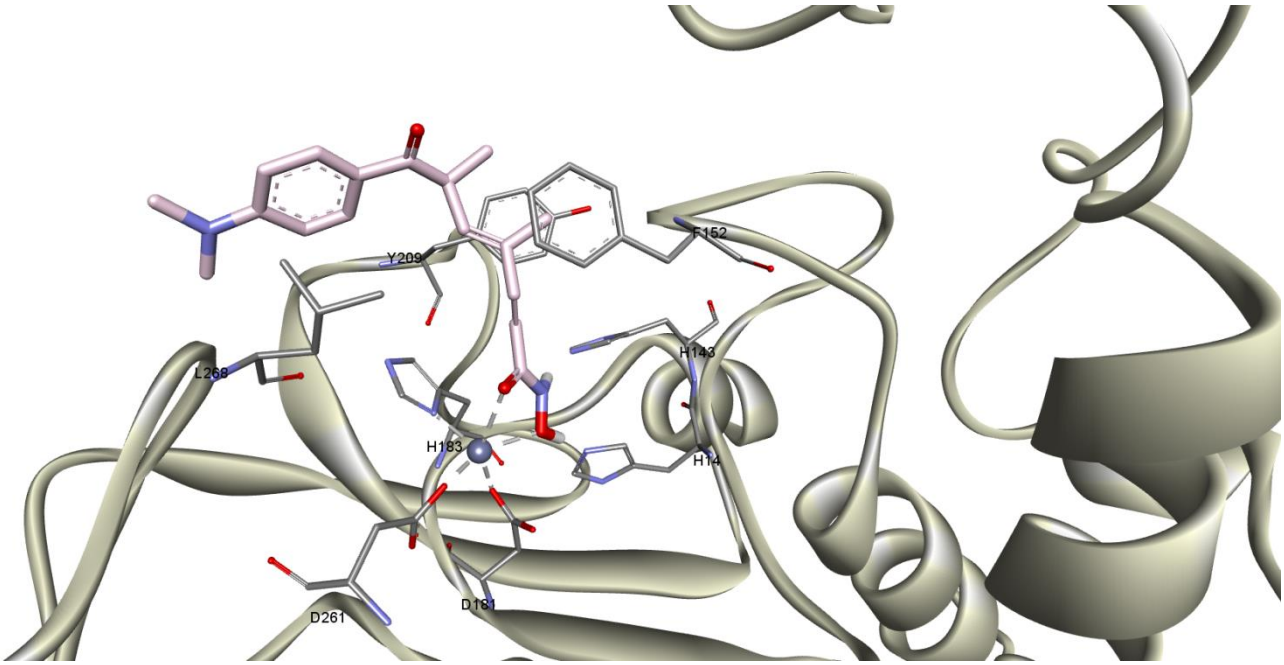

Figure S10

Position of ligand 18 inside the binding site of the HDAC1 seen from the extracellular side

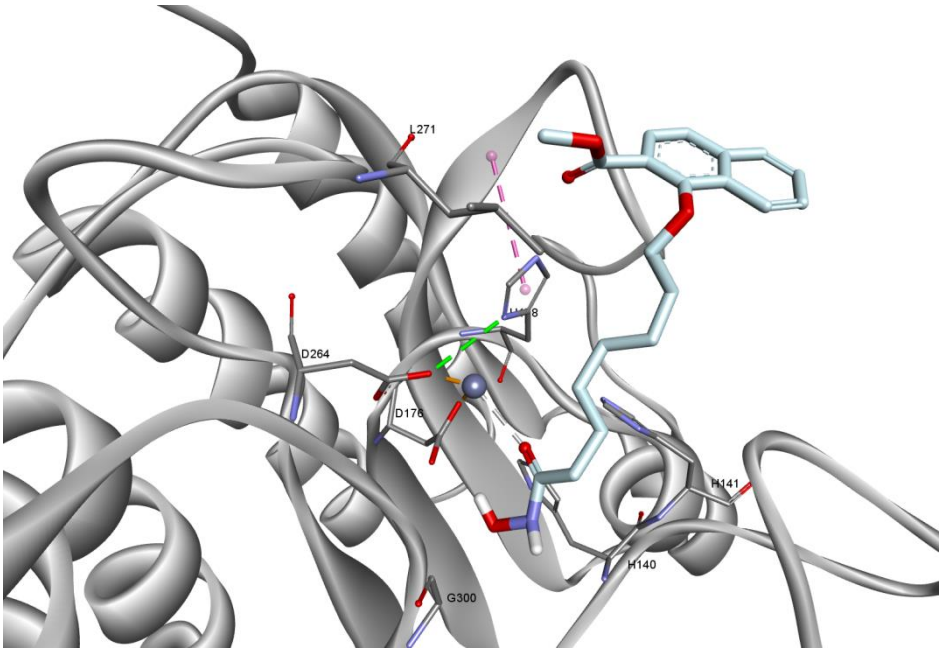

Figure S11

Position of ligand **18** inside the binding site of the HDAC2 seen from the extracellular side

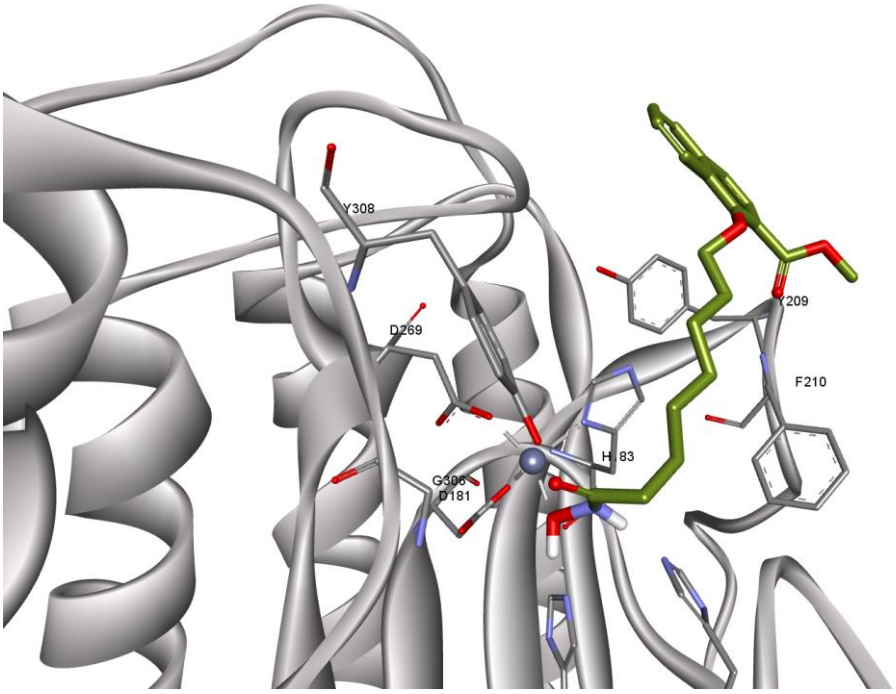

Figure S12

Position of ligand **18** inside the binding site of the HDAC3 seen from the extracellular side

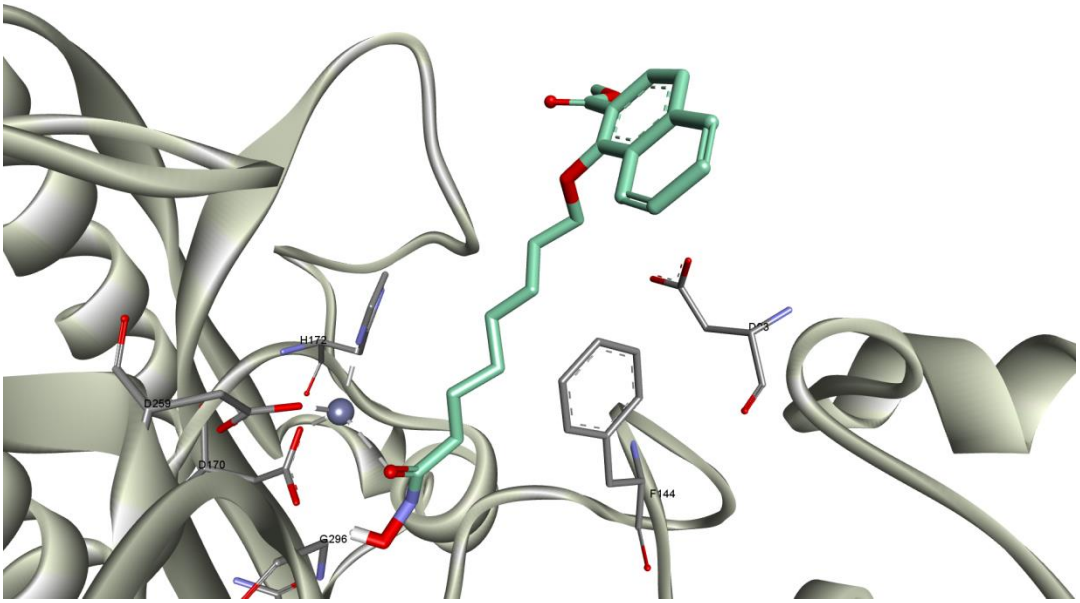

Figure S13

Position of ligand **18** inside the binding site of the HDAC4 seen from the extracellular side

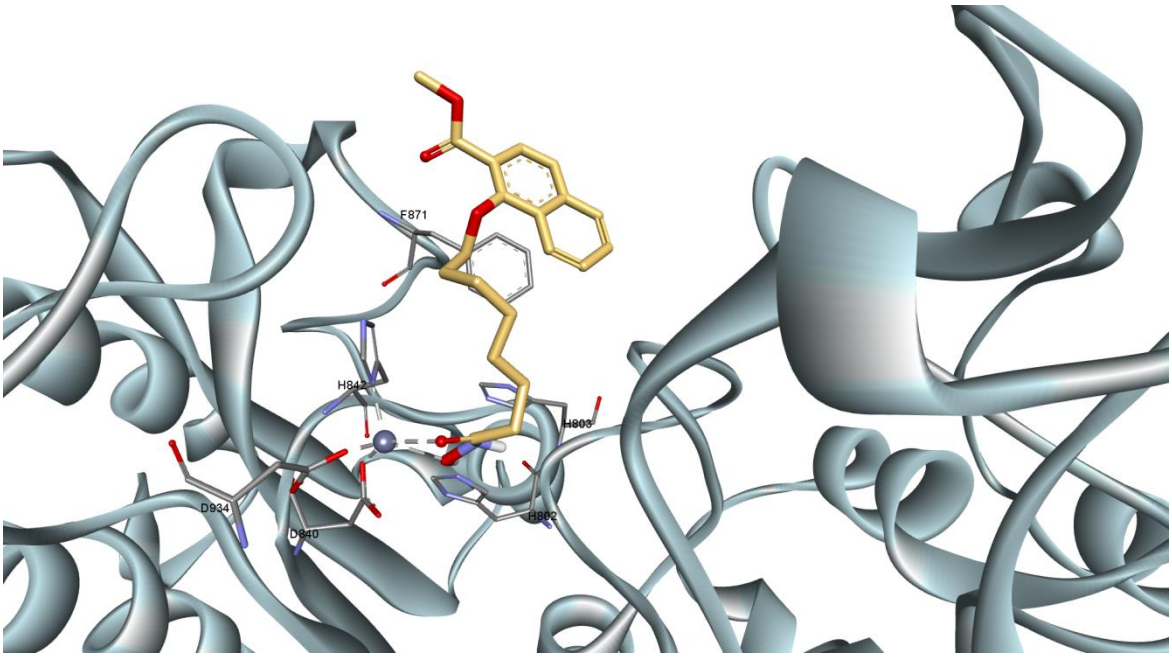

Figure S14

Different binding modes of ligand **18** inside the binding site of the HDAC5 seen from the extracellular side

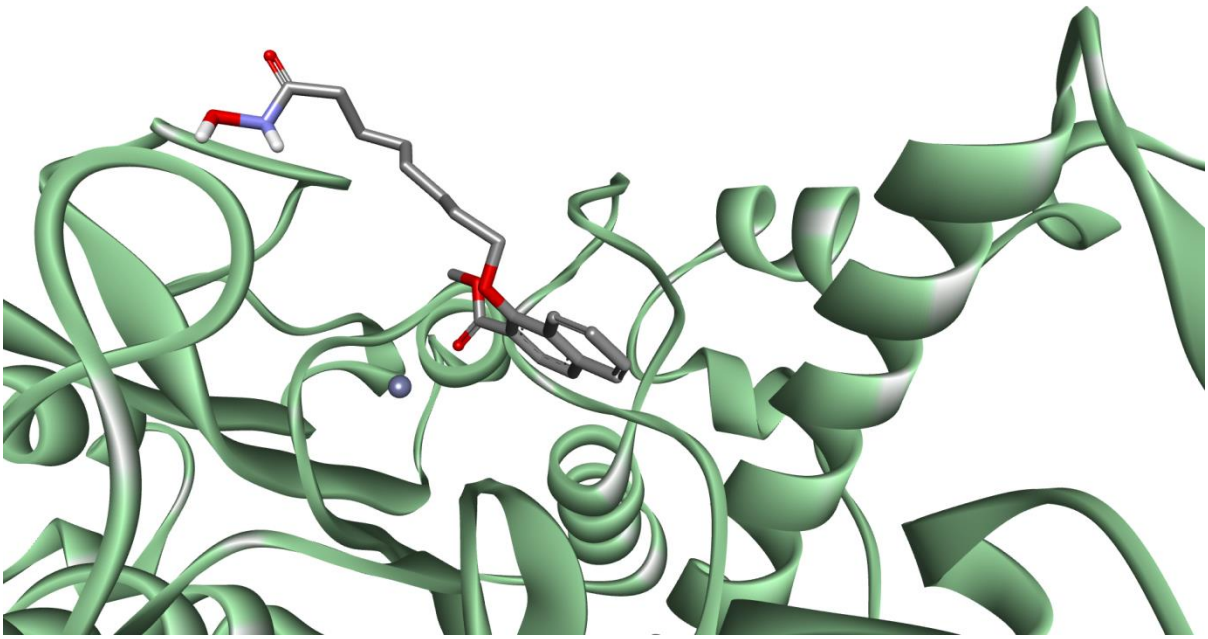

Figure S15

Position of ligand **18** inside the binding site of the HDAC6 (second catalytic domain) seen from the extracellular side

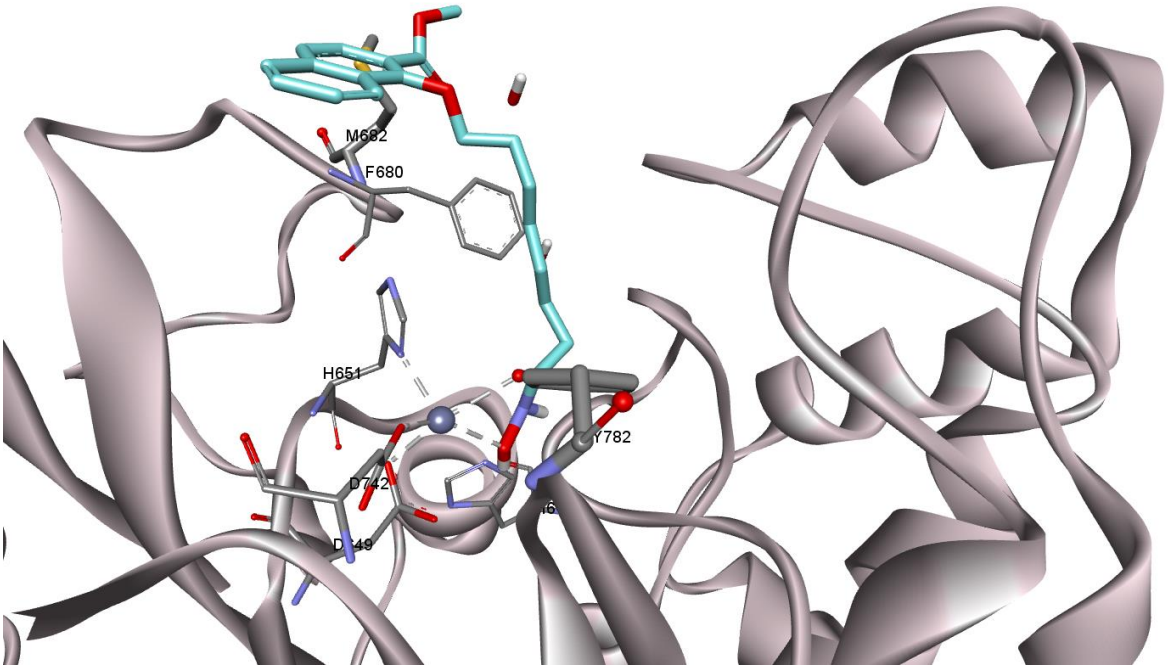

Figure S16

Different binding modes of ligand **18** inside the binding site of the HDAC7 seen from the extracellular side

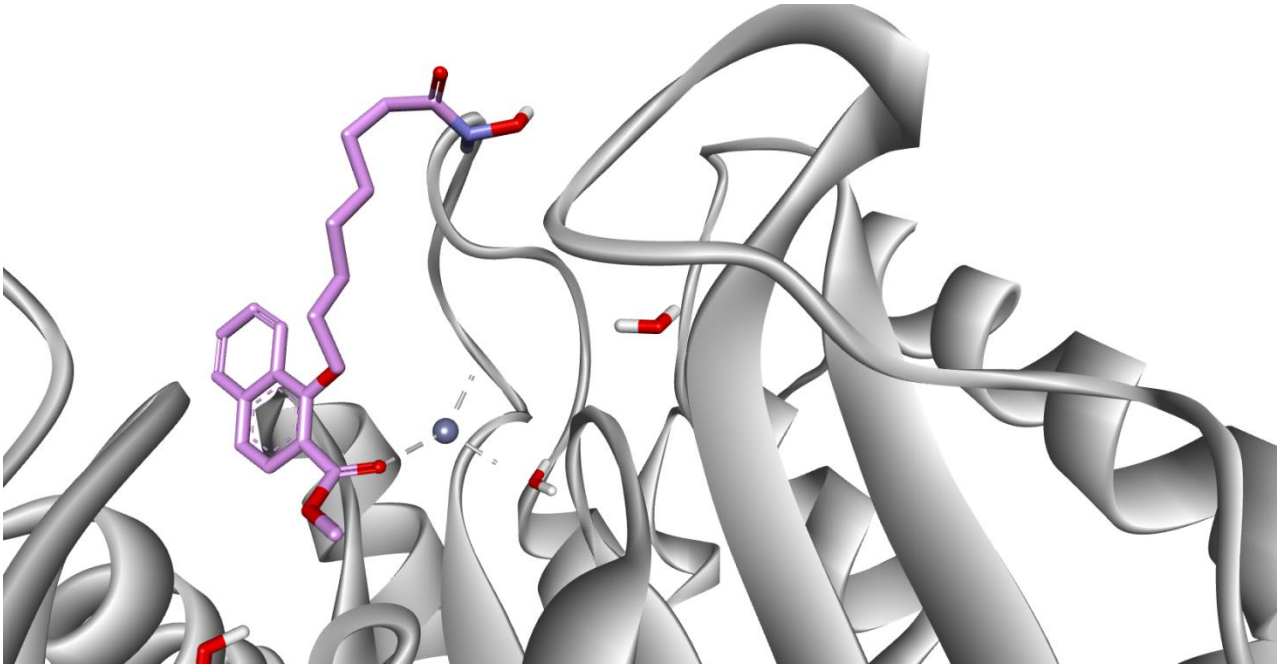

Figure S17

Position of ligand **18** inside the binding site of the HDAC8 seen from the extracellular side

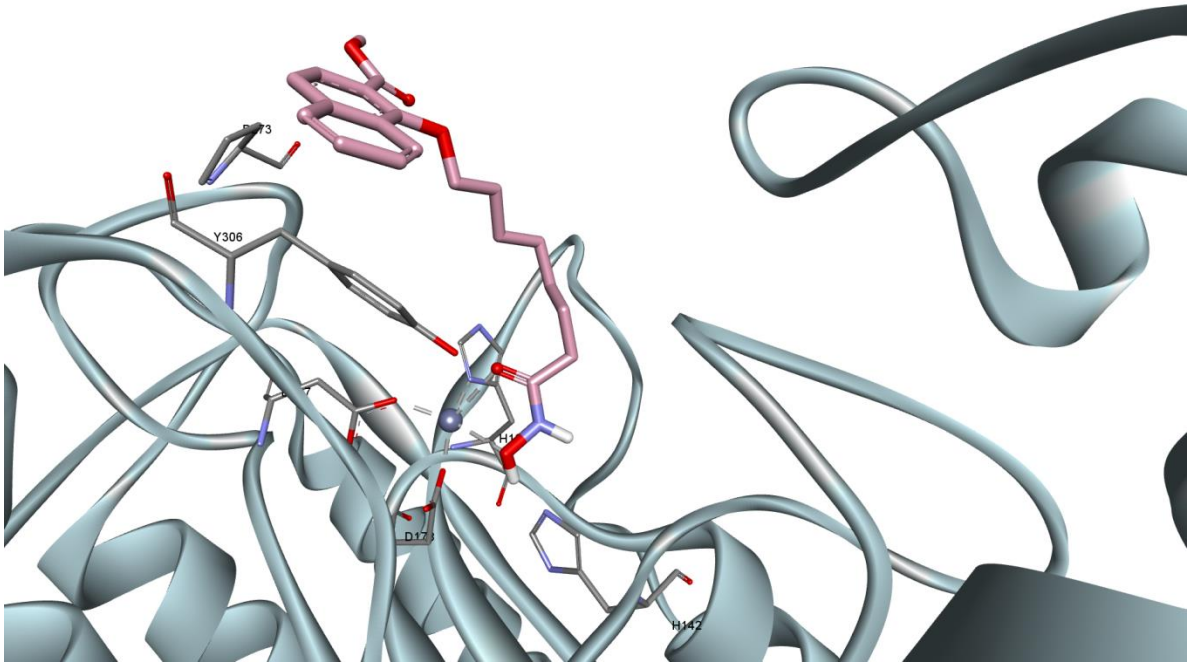

Figure S18

Position of ligand **18** inside the binding site of the HDAC9 seen from the extracellular side

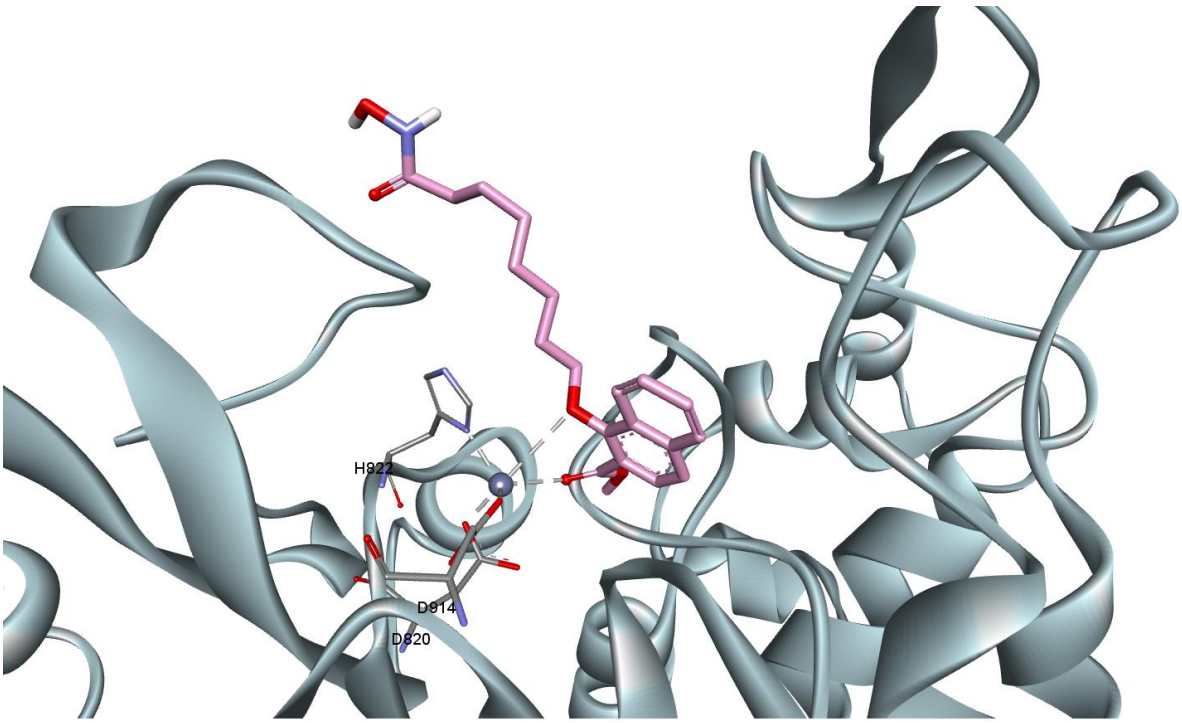

Figure S19

Position of ligand **18** inside the binding site of the HDAC10 seen from the extracellular side

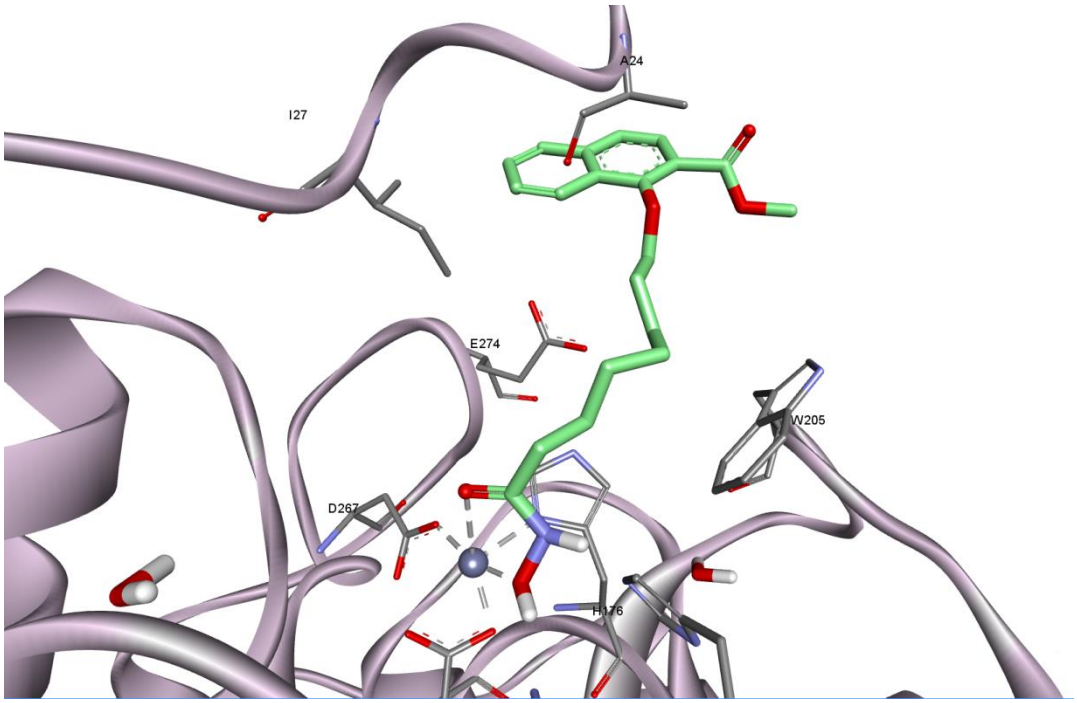

Figure S20

Position of ligand **18** inside the binding site of the HDAC11 seen from the extracellular side

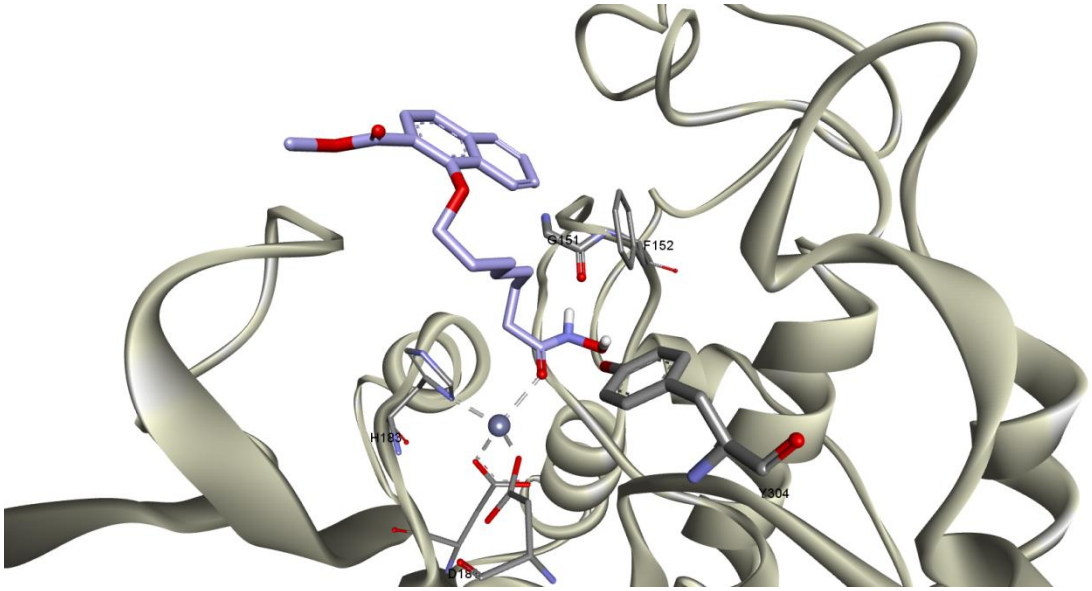

Figure S21

Position of ligand **18** inside the binding site of the HDAC6 (first catalytic domain) seen from the extracellular side

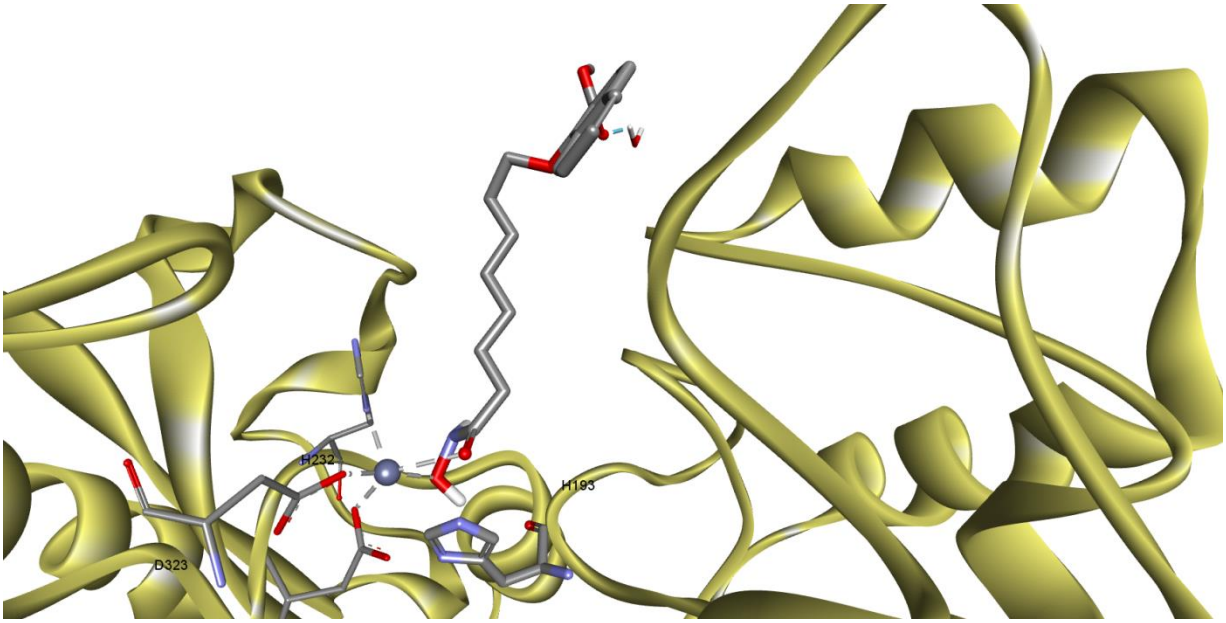

Atomic coordinates

They are provided in a separate zipped file containing the pdf files

[i] Miyake, Y.; Keusch, J. J.; Wang, L.; Saito, M.; Hess, D.; Wang, X.; Melancon, B. J.; Helquist, P.; Gut, H.; Matthias, P. *Nat Chem Biol* **2016**, *12*, 748–754.